International Workshop on Atomic Collisions and Atomic Spectroscopy with Slow Antiprotons (pbar99)

Book of Abstract

July 19-21, 1999
Tsurumi, Yokohama, Kanagawa, Japan

International Advisory Board:

J.Burgdoerfer, J.S.Cohen, R.Hayano, M.H.Holzscheiter, D.Horvath, M.Inokuti, H.Knudsen, K.Komaki, T.Yamazaki, Y.Yamazaki,

Organizing Committee: R.Hayano, H.Knudsen, K.Komaki, T.Yamazaki, Y.Yamazaki

Workshop Chairman: Ken-ichiro Komaki

Sponsor and Cosponsors

The Antimatter Science Project, University of Tokyo

The Center for CERN related Atomic and Nuclear Physics of the Danish Natural Science Research Council

R I K E N

Workshop Schedule & Site:

July 18th:
Welcome Drink: 19:30-21:30, Room "Sumire", 3rd floor of the New Tower of **Sinagawa Prince Hotel**
Registration Desk: 18:00-21:30, the same room as the Welcome Drink

July 19th:
Bus from Shinagawa Prince Hotel to Tsurumi Girls High School: 8:00
Registration Desk: 9:00-16:00, at **Tsurumi Girls High School**
Scientific Program: 9:00-16:00 at **Tsurumi Girls High School**
Social Program (Zazenkai): 16:10- at **Sojiji-Temple**
Bus from Tsurumi Girls High School to Shinagawa Prince Hotel (for those who do NOT join the Social Program at Sojiji): 16:10

July 20th:
Bus from Shinagawa Prince Hotel to Tsurumi Girls High School (for those who do not join the Social Program at Sojiji): 8:00
Registration Desk: 9:00-17:00, at **Tsurumi Girls High School**
Scientific Program:9:00-17:20 at **Tsurumi Girls High School**
Bus from Tsurumi Girls High School to Shinagawa Prince Hotel: 17:30
Workshop Banquet: 19:00-21:00 at Room "Aso", 6th floor of the New Tower of **Sinagawa Prince Hotel**

July 21st:
Scientific Program:9:00-12:30 at Room "Aso", 6th floor of the New Tower of **Sinagawa Prince Hotel**

Scientific Program

July 19th, morning session I:

K.Komaki (30min): Antimatter Science with Slow Antiprotons
H.Knudsen(30min): Experimental data on ionization and energy loss for antiprotons colliding with matter
P.Krstic (30min): Ionization of ions and atoms by slow antiprotons
A.Igarashi(15min): Ionization of atomic hydrogen with antiprotons

July 19th, morning session II:

R.Hayano (30min): Laser spectroscopy of protonium
J.S.Cohen (30min): Isotope effects on antiproton capture
M.Fujiwara (30min): Muon catalyzed fusion studies with a muonic hydrogen beam at TRIUMF
K.Ohtsuki (20min): Antiprotonic lithium atom $\bar{p}Li^{+}$; formation, energy levels and stability

July 19th, afternoon session:

K.Fine (40min): Nonneutral plasmas and antihydrogen production
T.Ichioka (30min): Status report on the ASACUSA antiproton trapping system
H.Totsuji (30min) : Two-Component Nonequilibrium Nonneutral Plasma in Penning-Malmberg Trap

July 20th, morning session I

M.Hori(30min): High-precision, two-photon laser spectroscopy of antiprotonic helium atoms and other experiments using ultra-low density targets
Y.Kino (30min): Non-Adiabatic High-Precision Calculation of Antiprotonic Helium Atomcule and Determination of Antiproton Mass
V. I.Korobov (30min): Spectroscopy of the antiprotonic atomcule
T.Koike(20min): Nuclear absorption process in antiprotonic helium atoms

July 20th, morning session II:

G.Ya.Korenman (30min): Collisions of antiprotonic atomcules with He atoms
D.Bakalov (30min): Density shift and broadening of the transition lines in antiprotonic helium
T.Azuma (20min) : Does a solvated antiproton exist ?

July 20th, afternoon session I:

H.Schmidt-Boecking (30min): Comparison of multi-differential ionization cross sections in fast antiproton and proton on Helium collisions --- A proposal for future studies with a table sized PBAR-storage ring
C.D.Lin (30min): Ionization of H and He atoms by antiprotons revisited
A.Kover (30min): Post Collision Interaction at Proton, Antiproton - Atom Collisions

July 20th, afternoon session II:

R.Schuch (20min): An accurate measurement of the p mass using highly charged ions in a Penning trap
E.Morenzoni (30min): A new low energetic muon beam and its applications
N.Kabachnik (20min): Channeling of slow antiprotons

July 21st, morning session I:

M.Holzscheiter (30min): Tests of CPT, Lorentz Invariance and the WEP with Antihydrogen
R.Schuch (20min): Making Hbar by recombination in a Penning trap
S.Schippers (30min): Recombination of H-like ions with electrons: a testing ground for the formation of anti-hydrogen?
P.Froelich (20min): Hydrogen - Antihydrogen Collisions

July 21st, morning session II:

Panel Discussion: Antihydrogen Production & Spectroscopy
M.Inokuti (20min): Concluding Remarks

Antimatter Science with Slow Antiprotons

K. Komaki

Institute of Physics, Graduate School of Arts and Sciences, University of Tokyo, 1-5-3 Komaba, Meguro-ku, Tokyo 153-8902, Japan

Experimental study in atomic physics using slow antiprotons used to be performed at LEAR, of which the main role was the exploration of exotic mesons. Since the shutdown of LEAR in 1996, much effort has been paid to construct a new facility dedicated to atomic physics. This effort has been realized as Antiproton Decelerator (AD) which is scheduled to be open for experiments in September, 1999.

Taking this opportunity, University of Tokyo members of former LEAR programs PS194, PS200 and PS205 joined to form a group, Antimatter Science Project, which aims at developing a new field of science, i.e., Antimetter Science, using slow antiprotons from AD. The group applied for a Grant-in-aid from the Japanese Ministry of Education, Science and Culture. The proposal was approved as a Grant-in-aid for Creative Basic Research(Shin-pro) which covers fiscal years from 1998 to 2002. The Shin-pro group and European group have organized an AD user group named ASACUSA(Atomic Spectroscopy And Collisions Using Slow Antiprotons).

The ASACUSA program consists of three phases, each of which is characterized by the energy region of available antiprotons. In phase 1 stage, 5.3-MeV antiprotons from AD are directly used and higher resolution spectroscopy of $\bar{p}He^+$ and new spectroscopy of hyperfine and superhyperfine structure of $\bar{p}He^+$ are the main experimental subjects. In phase 2, the AD beam is further decelerated by an RFQ post deceleration down to below 100 keV and stopping power measurement, channeling and swarm experiments using slow antiprotons are prepared. In phase 3, an electro-magnetic trap is to be installed downstream the RFQ to catch post-decelerated $\bar{p}$'s, to cool them down and to extract them as an ultra cold dc beam. Basic collision dynamics of $\bar{p}$'s, formation mechanism and spectroscopy of antiprotonic atoms are planned using the ultra cold $\bar{p}$ beam .

At the present stage, the preparation of the Phase 1 experiment, high precision laser and microwave spectroscopy of $\bar{p}He^+$ is almost completed. The construction of the RFQ post-decelerator, which is the main component of the Phase 2 facility, is getting ready for proton test at Aarhus. As for preparation of the phase 3, a superconducting magnet for the $\bar{p}$ trap has been constructed and the development of techniques for $\bar{p}$ trapping, cooling and extraction is underway using H^- ions.

Experimental data on ionization and energy loss for antiprotons colliding with matter

Helge Knudsen

Institute of Physics and Astronomy Aarhus University DK 8000 Aarhus C Denmark
hk@ifa.au.dk

During the decade where the LEAR accelerator at CERN existed, the PS194 collaboration obtained a substantial amount of experimental information on the interaction of antiprotons with matter in the impact energy range from 20 MeV to 13 keV. We concentrated on measurements of single - and multiple ionization cross sections of atoms and molecules, as well as the stopping power of several metals. These data spurred great interest among theorists, and much new knowledge concerning the basic dynamics of atomic collisions was obtained. In this talk I shall review the data as well as the theoretical advances. I shall also present our plans for future work in this field within the ASACUSA collaboration.

IONIZATION OF IONS AND ATOMS BY SLOW ANTIPROTONS

Predrag S. Krstic, David R. Schultz and Carlos O. Reinhold
Oak Ridge National Laboratory, Physics Division, P.O. Box 2008, Oak Ridge, TN 37831, USA

Introduction of antiprotons as projectiles in a heavy particle atomic collision process in both theory and experiment has yielded new and exciting physics by creating new reaction channels not previously seen in other collision processes. Although the Coulomb field of the antiproton is *per se* the same as that of an electron, the strong electron exchange effects in electron-atom collisions as well as the antiproton large mass make electron-atom and antiproton-atom collisions very different from each other, both phenomenologicaly and quantitatively. The negative charge of the heavy projectile has another consequence that distinguishes antiptoron-atom collisions from positive-ion - atom collisions: charge transfer of target electron(s) to the projectile is absent. As a consequence, any electron loss process is an ionization process, and if the energy is high enough, the later becomes the leading inelastic process.

When the velocity of the projectile is smaller than the Kepler orbiting velocity in the target atomic state, the system is in the so called adiabatic regime and inelastic processes can be best described as localized transitions between the quasimolecular adiabatic states. The localization of the transitions for positively charged ions can be associated with reaching the top of either the attractive potential barrier or the repulsive centrifugal barrier, which happens at the points of crossings of the molecular terms of the same symmetry in the plane of complex internuclear distance R, often called the hidden crossings. For antiprotons [1], the attractive potential barrier is missing and the former type of hidden crossings (Q-type), the source of so-called saddle point electrons in ionization becomes unimportant. The latter type of hidden crossings (spatially highly localized S-type) are not expected to be present with states of zero-angular momentum. A remarkable new feature of the topology of the adiabatic energy surfaces in collisions with antiprotons is the presence of an S-type series of hidden crossings even for zero-angular momentum states [2]. The analog of the repulsive centrifugal barrier here originates in the repulsive Coulomb potential between the antiproton and the target electron.

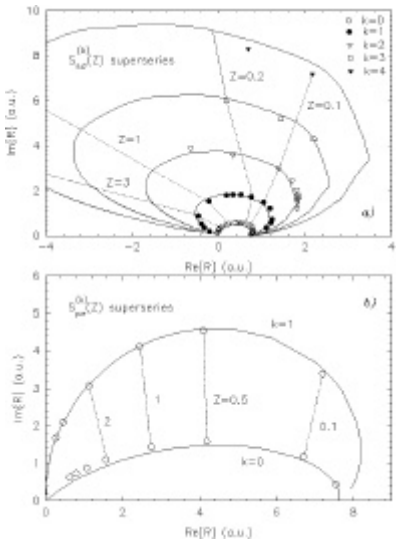

Figure 1 Position of the S-superseries limiting points for various orders k and target core charges z, Z=z-1, for a) s, and b) p initial states

Single electron ionization from the s-ground state proceeds entirely through S-promotion at very small internuclear distances and is caused by the antiproton repulsion. Figure 1 displays the topology of the S-promotion series for various target core charges and, thus, contains all information needed to understand single electron ionization for antiproton-ion slowly colliding systems [1].

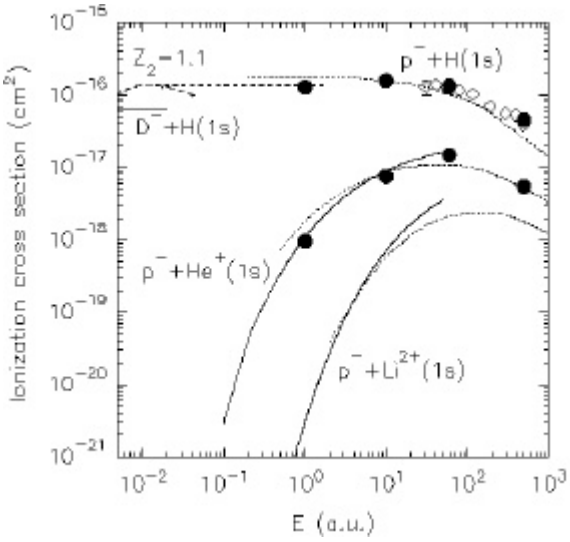

Figure 2 The cross section for ionization of hydrogen and hydrogenic ions in collisions with antiprotons

Figure 2 shows the ionization cross sections for several systems calculated with the hidden-crossings method (full lines). We also performed calculations using a direct solution of the time dependent Schroedinger equation (TDSE) (black circles) which confirms the physical picture of the processes as described above. The antiproton-hydrogen system provides an exemption to this picture [2]. In this case, at internuclear distances smaller than the Fermi-Teller limit (R_{FT}=0.6394 a.u.) the Coulomb field of the proton-antiproton electric dipole cannot support any bound state. As a consequence, all quasimolecular s-states merge with the continuum edge at $R=R_{FT}$ and the S series of hidden crossings collapses to the real axis (Figure 1). Thus, the system looses its adiabatic promotion properties and ionization must be described by diabatic methods even at the lowest collision energies. Our TDSE treatment solves the controversy [2] on the behavior of the ionization cross sections at low energies (Figure 2), confirming previous CTMC predictions [3], and disagreeing with the CDW results [2]. Like other perturbative methods, the latter approach does not take into account the strong quasimolecular deformation of the system with R and thus greatly underestimates the ionization cross section.

Ionization of He by antiproton impact resembles that for the p^-+H system since the quasimolecular energies are also strongly deformed at small internuclear distances. In this case, however, the ground term approaches closely rather than merges with the single ionization continuum (for R=0 the system goes to H^-, which is only 0.0257 a.u. below the ionization continuum). Thus, one can expect that the single electron ionization happens somewhere between R=0.2 a.u. (where p^-+He^+ ionizes) and R_{FT}. In previous calculations [4], using the multielectron hidden crossings theory [5], we found a hidden crossing at R_c=0.62 a.u. leading to single electron ionization (MEHC in Fig.3). The disagreement between FIM calculations [6] and our calculations with experiment [7] is not completely understood. Theoretically, there exists a possibility that our calculation is not converged (we used a truncated basis expansion for this nonseparable problem). The lack of a full treatment of electron correlation effects (we used only

singly excited CI states) may also be a possible cause of disagreement [4]. Thus, a new algorithm has been developed, which fully accounts for correlation effects and the convergence has been greatly improved in the plane of complex R by a variational optimization of the Slatter basis exponents. The new results, to be shown at the meeting highlight the nonadiabaticity of the problem (small single-electron binding energies at small internuclear energies) as a main cause of the difficulties to reach a correct result. Thus, the adiabatic treatment is replaced by a diabatic one. In addition, we generalized the TDSE method to four dimensions, adapting the time-dependent treatment to a two-dimensional antiproton-helium collision system.

Double ionization of He by antiproton impact is a more standard problem. Theoretical and experimental results for this channel are in relatively good agreement [4] and there is not much controversy. The ionization goes dominantly through sequential one-electron channels, but we found a nonnegligible contribution of the highly correlated simultaneous two-electron ionization. This is realized through a new series of hidden crossings which connects doubly excited helium states.

We gratefully ackowledge support from US DOE, Office of Fusion Energy Sciences and Office of Basic Energy Sciences through ORNL, managed by Lockheed Martin Energy Research Corporation under contract No. DE-AC05-96OR22464.

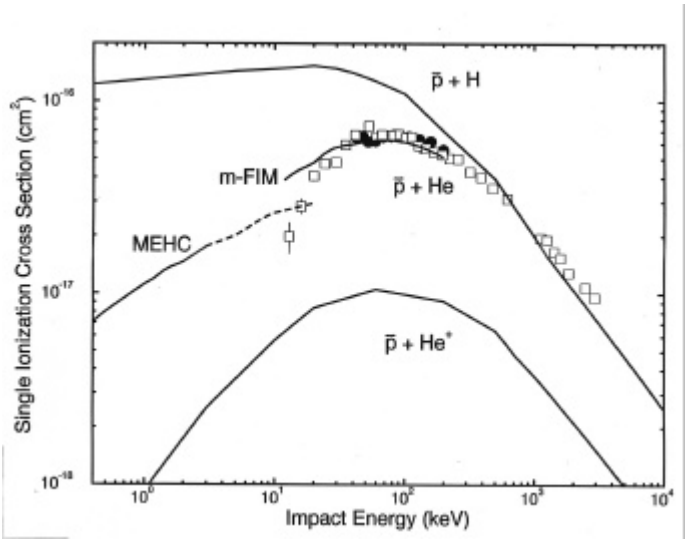

Figure 3 Single ionization of H, He and He^+ in collisions with antiprotons. Symbols are explained in the text.

References:

1. P.S. Krstic, D.R. Schultz and R.K. Janev, J. Phys. B 29, 1941 (1996).
2. D.R. Schultz, P.S. Krstic, C.O. Reinhold, and J.C. Wells, Phys. Rev. Lett. 76, 2882 (1996).
3. D.R. Schultz, Phys. Rev. A 40, 2330 (1989).
4. G. Bent, P.S. Krstic and D.R. Schultz, J. Chem. Phys. 108, 1459 (1998).
5. P.S. Krstic, G. Bent and D.R. Schultz, Phys. Rev. Lett. 77, 2428 (1996).
6. J.F. Reading et al, J. Phys. B 30, L189 (1997).
7. P. Hvelpund, H. Knudsen, U. Mikkelson, E. Morenzoni, S.P. Moller, E. Uggerhoj, and T. Worm, J. Phys. B 27, 925 (1994).

Ionization of atomic hydrogen with antiprotons

A. Igarashi
Faculty of Engineering, Miyazaki University, Miyazaki, 889-2192, Japan

The collision of antiprotons $\bar{p}$ with atomic hydrogen is important as the simplest system where a heavy negative-charged particle collides with an atom. For collision energies below the ionization threshold, the protonium ($\bar{p}p$) formation is dominant, which is very difficult to treat from the theoretical point of view. In the present work, we consider collision energies above 1 keV where the protonium formation is negligible and the impact parameter method is valid. Since the electron capture does not occur in the case of $\bar{p}$ impact which greatly differs from the p impact, the expansion of the wavefunction in terms of atomic orbitals centered on only proton is likely to work well. While such a calculations was reported by Hall et al[1], we will develop a similar calculation with larger basis and compare the cross sections with existing calculations [2-5]. The differential cross sections (DCS) with respect to ejected electron momentum will also be shown.

In the impact parameter method, the internucler motion is classically treated as $\mathbf{R} = \mathbf{b} + \mathbf{v}t$ with impact parameter $\mathbf{b}$, the collision velocity $\mathbf{v}$, which is taken to be perpendicular to $\mathbf{b}$, and time t. The total wavefunction at impact parameter $\mathbf{b}$ and time t is the solution of the time dependent Shorödinger equation

$$\left(h + V(\mathbf{r}, \mathbf{R}) - i\frac{d}{dt}\right)\Psi(\mathbf{r}, t) = 0, \qquad (1)$$

where r is the position vector of the electron from p, h Hamiltonian of H, and V is the interaction between $\bar{p}$ and H.

The total wavefunction is expanded as

$$\Psi = \sum_i c_i(t)\phi_i(\mathbf{r})\exp(-i\epsilon_i t). \qquad (2)$$

Here ϕ_i is an atomic orbital with energy ϵ_i and c_i is the expansion coefficient. The atomic orbitals are prepared by diagonalizing h in Eq. (1) in terms of Sturmian orbitals. Substitution of Eq. (2) into the Shrödinger equation (1), we have coupled equations with respect to the expansion coefficients,

$$i\frac{d}{dt}c_i = \sum_j \exp(i(\epsilon_i - \epsilon_j)t) < \phi_i|V|\phi_j > c_j. \qquad (3)$$

The transition amplitude at impact parameter b is defined as $c_i(+\infty)$ by solving the above equations with the initial condition $c_i(-\infty) = \delta_{i,1s}$.

Though the total ionization cross sections is obtained as a sum of excitation cross sections into the states with positive energies in terms of an expansion involving pseudo states, $d\sigma/d\mathbf{k}$ can not be obtained. For that, we apply the integration form

$$T_{\mathbf{k}}(\mathbf{b}) = -i\int_{-\infty}^{+\infty} dt < \exp(-i\epsilon_{\mathbf{k}}t)\phi_{\mathbf{k}}|V|\Psi >, \qquad (4)$$

where $\phi_{\mathbf{k}}$ is the coulomb wavefunction and Ψ is approximated by the wavefunction in Eq. (2).

Fig.1 is the total ionization cross section. The 265 orbitals up to $\ell = 5$ are coupled in the coupled equations. While this basis seems to be insufficient for lower energies, the agreement with other calculations is satisfactory.

Fig.2 is the DCS with respect to the electron ejection angle of $p, \bar{p}$ impacts at 100 keV. The proton impact has large DCS in the forward direction, while the DCS at larger angles are enhanced for $\bar{p}$ case.

Fig.1

Measurement:
Knudsen et al.[6] (•).
Calculations:
Present (×).
Hall et al.[1] (○).
Schultz et al. [3](◇).
CDW-EIS
(dashed curve).

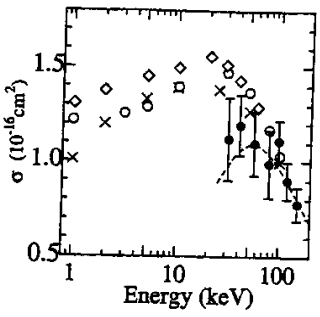

Fig.2

Present (solid curve)
CDW-EIS
(dashed curve)

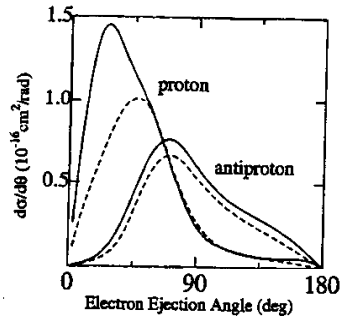

References

1. K. A. Hall et al, JPB **29**, 61232 (1996).
2. A. M. Ermoraev, Hyperfine Interact. **44**, 375 (1988).
3. D. R. Schultz et al, PRL **76**, 2882 (1996).
4. J. C. Wells et al, PRA **54** 593 (1996).
5. P. S. Krstić et al, JPB **29**, 1941 (1996).
6. H. Knudsen et al, PRL **74** 4627 (1995).

Laser Spectroscopy of Protonium

R.S. Hayano
Department of Physics, University of Tokyo,
7-3-1 Hongo, Bunkyo-ku, Tokyo 113-0033, Japan

Production of ultra-slow $\bar{\mathrm{p}}$ beam and its use for atomic collision and spectroscopy studies are important goals of ASACUSA collaboration at AD. We plan to decelerate the 5.3 MeV beam from AD to $10 \sim 50$ keV with a radio frequency quadruple (RFQ) decelerator, and then inject this beam further into a $\bar{\mathrm{p}}$ catching trap similar to the PS200 trap at LEAR. Antiprotons will be cooled in the trap by the electron-cooling technique, and then extracted at very low energies of $1 \sim 100$ eV.

With such an ultra low energy $\bar{\mathrm{p}}$ beam, many new experiments will become possible, and production and spectroscopy of protonium ($\bar{\mathrm{p}}\mathrm{p}$) in a near-vacuum condition is one of the interesting possibilities. It is well known that protoniums produced in gaseous hydrogen are quickly quenched by Stark collisions. However, if we can make protoniums in vacuum, for example by colliding ultra-slow $\bar{\mathrm{p}}$'s on an atomic gas jet target, protoniums can only deexcite by slow radiative transitions, and should be quite long lived. The radiative lifetimes exceed 1 μs for near-circular states for $n \sim 30$, and exceed 100 μs for $n \sim 80$. Such metastable antiprotonic atoms can be studied in detail by using high-precision laser spectroscopy techniques. Of course, such experiments with protoniums are practically impossible at present due to the lack of high-intensity ultra-slow $\bar{\mathrm{p}}$ beams.

A possible scheme to carry out the laser spectroscopy of protonium comprises the following steps:

1. Ultra slow antiprotons ($E_{\bar{p}} \sim 30$ eV) are extracted from a catching trap, hit an atomic hydrogen gas target and form protoniums. The kinetic energy of antiproton is adjusted to populate $n \sim 40$ for which the lifetime is a few microseconds. The density of the atomic target is low enough so that Stark collisions, which is the dominant quenching process in H_2 target, are unimportant.
2. Protoniums are selectively excited by two counter-propagating laser beams to $n \sim 80$.
3. On-resonance protoniums survive the 1 m flight path ($\sim 30\mu$s flight time) and are detected with the annihilation detector placed at the end of the flight path, but off-resonance protoniums annihilate in flight and do not reach the detector. By counting the number of protonium arriving at the detector as a function of laser frequency, we can determine the protonium energy level spacings.

This is an interesting challenge which, if successfull, would make it possible to improve the precision of the "(anti)protonic Rydberg" constant.

Abstract for International Workshop on Atomic Collisions
and Atomic Spectroscopy with Slow Antiprotons
July 19–21, 1999

Isotope Effects on Antiproton Capture

James S. Cohen

Theoretical Division, Los Alamos National Laboratory,
Los Alamos, New Mexico 87545, USA

Cross sections for capture of the antiproton ($\bar{p}$) and negative muon (μ^-) by the H_2 and D_2 molecules have been calculated using fermion molecular dynamics (FMD). All the cross sections are significantly larger than those for capture by the corresponding atom, also evaluated by the FMD method. The largest molecular cross sections are obtained when the negative projectile mass best matches the nuclear mass in the molecular target, thus for $\bar{p}$+H_2. The vibrational degree of freedom is shown to be most important in distinguishing the four reactions, but the effects of rotations, two-center electronic charge distribution, and nonadiabaticity are also significant. The predicted *initial* capture fractions (i.e., not taking subsequent transfer into account) in a H_2/D_2 mixture are $P^{(p)}_{\rm capt}/P^{(d)}_{\rm capt} = qc_p/c_d$, where $q = 1.585$ for $\bar{p}$ and $q = 1.186$ for μ^- independent of c_p and c_d. It is expected that the antiproton cross sections will be measured for the first time by the ASACUSA Collaboration at the new Antiproton Decelerator (AD) being built at CERN.

The n and l distributions of the exotic atoms formed with molecular targets are found to be quite different from those found for atomic targets. In the case of the molecular targets, the maxima of both the n and l distributions are shifted to lower values and the very large n values are suppressed. These quantum-number differences between atomic and molecular targets are due to the molecular geometry as well as the breakup dynamics of the intermediate complex formed in molecular capture. The quantum-number difference between the two molecular isotopes is mainly a reduced-mass effect, as it is for the different atomic isotopes.

Using the same method, cross sections for negative pion capture by H_2, D_2, and HD have also been calculated. With these cross sections, the reduced capture ratio for a H_2+D_2 mixture is found to be $(P_p^{(H_2+D_2)}/P_d^{(H_2+D_2)})/(c_p/c_d) = 1.204$, and the capture ratio for HD is found to be $P_p^{(HD)}/P_d^{(HD)} = 0.875$. In light of these results, the p-to-d pion transfer probabilities Q are reevaluated using prior experimental data and determined to be larger than previously thought: $Q = 0.28$ at deuterium fraction $c_d = 0.5$ and $Q = 0.42$ as $c_d \to 1$. The puzzling relationship of the experimental data for HD to that for H_2+D_2 mixtures is explained.

Muon Catalyzed Fusion Studies with a Muonic Hydrogen Beam at TRIUMF

M.C. Fujiwara,[a]1 J.M. Bailey,[b] G.A. Beer,[c] J.L. Beveridge,[d] M. Faifman,[e] T.M. Huber,[f] R. Jacot-Guillarmod,[g] P. Kammel,[h] P.E. Knowles,[c,g] S.K. Kim,[i] A.R. Kunselman,[j] M. Maier,[c] V.E. Markushin,[k] G.M. Marshall,[d] C.J. Martoff,[l] G.R. Mason,[c] F. Mulhauser,[g] A. Olin,[d] C. Petitjean,[k] T.A. Porcelli,[c]2 and J. Zmeskal[m]

TRIUMF Muonic Hydrogen Collaboration

[a] University of British Columbia, Canada, [b] Chester Technology, UK, [c] University of Victoria, Canada, [d] TRIUMF, Canada, [e] Russian Research Center, Kurchatov Institute, Russia, [f] Gustavus Adolphus College, USA, [g] Université de Fribourg, Switzerland, [h] University of California at Berkeley & LBNL, USA, [i] Jeonbuk National University, Korea, [j] University of Wyoming, USA, [k] Temple University, USA, [l] PSI, Switzerland, [m] Austrian Academy of Sciences, Austria

Muon catalyzed fusion (μCF) is interesting not only because of potential applications, but also because it presents fundamental few-body problems involving the interplay of strong, electromagnetic and weak interactions. At TRIUMF, we have studied various muonic reactions with a unique target system using cold films of solid hydrogen isotopes. Exploiting a fortuitous effect in the muonic three-body interaction known as the Ramsauer-Townsend (RT) effect, muonic tritium (μt) can be extracted from the layer, providing a slow neutral beam of exotic atom. By placing a second interaction layer, separated by drift distance in vacuum, reaction cross sections can be measured on event-by-event basis, and the time of flight can provide energy-dependent information. This is in sharp contrast to conventional methods where a muon is stopped in a bulk gas or liquid target in which complex interconnected chains of reactions take place. The use of the muonic atom beam thus enables us to isolate the process of interest.

We will discuss some of our recent results which include: (1) time-of-flight measurement of μt scattering on protons, providing spectroscopic evidence for the existence of the RT effect. (2) a quantitative test of theoretical cross sections for μt deceleration on deuterons, where our sensitivity to the scattering angular dependence suggested the importance of the p-wave contribution. (3) direct confirmation of the existence of strong resonance in $d\mu t$ molecular formation at epithermal energies, in which the rate for this key process was measured to be nearly two orders of magnitude larger than previously observed at lower temperatures. (4) test of three-body calculations for the formation resonance energies, with our experimental accuracy approaching the magnitude of vacuum polarization and other QED effects.

---

[1] Present address: Department of Physics, University of Tokyo, Japan

[2] Present address: University of Northern British Columbia, Canada

Antiprotonic lithium atom $\bar{p}Li^+$; formation, energy levels and stability

Kazumasa Ohtsuki,
Univ. of Electro-Communications,
Chofu, Tokyo 182-8585, Japan

Nowadays, none may doubt the scenario for the long-lived antiproton in helium atoms as follows;

1) a slow antiproton collides with a helium atom, then one of the $1s$ electron oozes out into a continuum state with a low kinetic energy and the antiproton is captured simultaneously into a quasi-bound orbital in the potential of He^+. Almost of the states for $\bar{p}He^+$ atom are not stable for the fast Auger transition and the rest $1s$ electron is ejected into a continuum state so quickly. For some of the states having a higher angular momentum L (the same as rotational quantum numbers J in the molecular model), however, the Auger transition rate are less than the radiative transition rate.

2) An antiproton occupies a orbital of which the Auger transition is suppressed may deexcite primary by the radiative emission, typical life times of which are of the order of microseconds. During the deexcitation process by the radiative emission, the annihilation of an antiproton and a proton does not occur. (Once the Auger transition happens after several emissions of the radiation a $\bar{p}$ even in a higher angular momentum state would be absorbed immediately into the nuclei He^{2+} through the s-channel due to the Stark mixing because of the degeneracy of the hydrogenic $\bar{p}He^{2+}$ level structure.)

The long-lived antiproton has never been observed in any atoms or molecules other than helium atom while do in any phases (gas, liquid and solid) of helium atom in which frequent collisions of a $\bar{p}He^+$ with ambient helium atoms may be expected.

In the theoretical point of view, as quasi-bound orbitals for $\bar{p}$ moving around a singly charged ion A^+, infinite series with any number of angular momentums are possible because of the nature of atomic-like orbitals in the attractive Coulomb potential. This leads to a natural conclusion that the metastable states of an antiproton against the fast Auger transition do exist in any antiprotonic atoms $\bar{p}A^+$.

As the final states of the Auger decay for the initial states of $\bar{p}A^+$, an angular momentum L' of the $\bar{p}$ in $\bar{p}A^{2+}$ must be smaller than the critical value of L'_c since the energy of $\bar{p}A^{2+}$ with $N' \geq L'_c + 2$ are higher than that of A^+. Such states of $\bar{p}A^{2+}$ are never considered as the Auger decay channels for $\bar{p}A^+$. If the difference of $L - L'_c (\geq 0)$ is large enough, the Auger transition may extremely be suppressed. Of course, such a highly excited $\bar{p}A^+$ atom could not be stable for the collision of $\bar{p}A^+$ with A but such collisions would be removed if the single-collision experiments were performed.

In the prediction of the metastable (nearly stable) states described above, the formation process of $\bar{p}A^+$ due to the collision of a $\bar{p}$ with an A is not taken into account. To discuss the long-lived antiproton in atoms we have to consider the followings ;

1) the states of $\bar{p}A^+$ with the energy values within the range from A to A^+,

2) the critical angular momentum L'_c of $\bar{p}A^{2+}$ as the Auger decay channel,

3) Possibility of the population for the state $\bar{p}A^+$ due to the collision of $\bar{p} + A$ as a function of L.

In this sense, the long-lived antiproton in lithium atom is studied in this work.

All of numerical procedures are based on the Born-Oppenheimer approximation in this work. The exact electronic wave function for $\bar{p}Li^{2+}$ is obtained, while the configuration interaction (CI) calculations are done to obtain energies and wave functions for both multi-electron systems of $\bar{p}Li^+$ and $\bar{p}Li$ using multi-centered Slater-type functions.

Figure 1 shows the adiabatic potential energy curves for $\bar{p}Li^+$ with angular momentum numbers $62 \leq L \leq 66$ and $\bar{p}Li^{2+}$ for $L' = 37$ and 38. In the formation process of $\bar{p}Li^+$, if the kinetic energy ϵ of escaped electron is negligibly smaller than the ionization potential of lithium atom (5.4 eV), the energy levels of formed $\bar{p}Li^+$ are expected to lay above the dot line of the ground-state of Li atom. In such a case, the lowest level for $\bar{p}Li^+$ populated in the collision of $\bar{p} + Li$, the corresponding its principal quantum number N_0 called "the most probable N", is expected to be 64 or 65.

Meanwhile, in the adiabatic potential energy curves for $\bar{p}Li^{2+}$ with angular momentum $L' = 37$ and 38, it is found that the state with $N' = 38, L' = 37 (v' = 0, J' = 37)$ is the Auger decay channel with the highest angular momentum for the states of $\bar{p}Li^+$ with $L \geq 37$. This leads to an significant speculation with respect to the Auger decay rate of $\bar{p}Li^+$. As an example, for $\bar{p}Li^+$ in the state of $(N, L) = (65, 64)$ the Auger transition requires that one of the $1s$ electrons jumps into a continuum state with an angular momentum at least $l_e \geq 28$. The rate of transitions with such a huge angular momentum transfer from an antiproton to an electron are expected to be nearly zero.

The energy levels of $\bar{p}\mathrm{Li}^+$ in Figure 2 are shown for the states of $62 \leq N \leq 67$ and $55 \leq L \leq 66$. For all of such states, it is considered that a $\bar{p}$ is moving around the outside of the $1s$ electron's cloud. The energy sublevels of $\bar{p}\mathrm{Li}^+$ with the same N, in contrast to the case of a protonium $p\bar{p}$, are not degenerated. This level structure indicates that the nuclear absorption of a $\bar{p}$ due to the Stark mixing is also negligible for $\bar{p}\mathrm{Li}^+$.

Figure 2 also shows the energy level spacings of $\bar{p}\mathrm{Li}^+$, typical transition energies for $\Delta N = 1$ are of $0.15 \sim 0.19$ eV which are in the region of the infrared ray as the usual molecules. These level spacings indicate that the radiative transition rates of $\bar{p}\mathrm{Li}^+$ are quite small as compared with those of $\bar{p}\mathrm{He}^+$ being almost a few eV since the radiative transition rates are proportional to ΔE^3.

In the Born-Oppenheimer approximation, an antiproton capture by a lithium atom having one valence electron such as $\bar{p} + \mathrm{H}$ is described well by the theory of the electronic state in the potential of a permanent dipole moment consists of $\bar{p} + \mathrm{A}^+$. It is also applicable to the collisions of a $\bar{p}$ with a singly exited atom A^*. In a stationary dipole moment of a system $\bar{p} + \mathrm{A}^+$, any member of an infinite series of bound $ns - \sigma$ states do exist if the magnitude of a dipole moment is larger than the so-called critical dipole moment of 0.639 (in a.u.). For the case of $\bar{p}\mathrm{Li}^+$, the nuclear distance defined as R_c which provides the critical dipole moment is nearly $0.795a_0$. In the first order approximation, the valence electron $2s\sigma$ will ooze out when the nuclear distance R is less than R_c. Such a electron emission process is well known as the adiabatic ionization. If the initial kinetic energy of the projectile $\bar{p}$ (in c.m.) is lower than the ionization potential of lithium atom then the formation of an antiprotonic lithium atom may occur.

The adiabatic potentials for $\bar{p} + \mathrm{Li}^+$ and $\bar{p} + \mathrm{Li}$ with angular momentums $62 \leq L \leq 66$ are shown in Figure 3. Repulsive centrifugal potentials in the nuclear distance of $R \geq 4a_0$ are small enough for a slow antiproton to penetrate into the $2s\sigma$ electron's cloud. Figure 3 also shows the potential barriers at $R \leq 2a_0$ which prevent the antiproton from reaching to the critical distance R_c, thus the adiabatic ionization is impossible for such angular momentums. However, the non-adiabatic transition of the $2s\sigma$ electron to a continuum state is expected to play an important role in that region of R. In the formation of $\bar{p}\mathrm{He}^+$, the non-adiabatic transition must be essential because the electronic energies of $\bar{p} + \mathrm{He}$ are always lower than those of $\bar{p} + \mathrm{He}^+$ in any nuclear distances, even in the limit of $R \to 0$ where $\bar{p} + \mathrm{He} \to \mathrm{H}^-$ and $\bar{p} + \mathrm{He}^+ \to \mathrm{H}$.

All of the theoretical results suggest that $\bar{p}\mathrm{Li}^+$ will have the longest life time among all of antiprotonic atoms in the "vaccume". Details are going to be presented in the workshop.

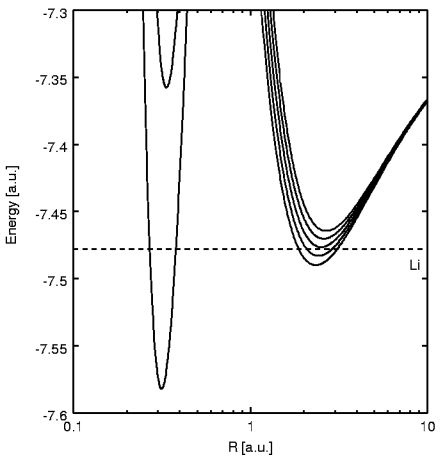

Figure 1: Adiabatic potentials for $\bar{p}\mathrm{Li}^+$ with $62 \leq L \leq 66$ and $\bar{p}\mathrm{Li}^{2+}$ with $L' = 37, 38$. The dot line indicates the energy level of the ground state of Li atom. Horizontal axis is represented in logarithmic.

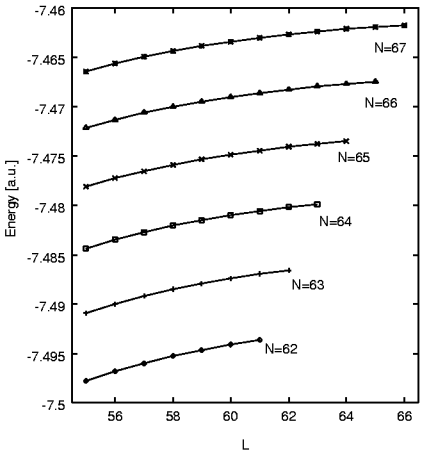

Figure 2: Calculated energy levels of $\bar{p}\mathrm{Li}^+$ for the states of $62 \leq N \leq 67$ and $55 \leq L \leq 66$.

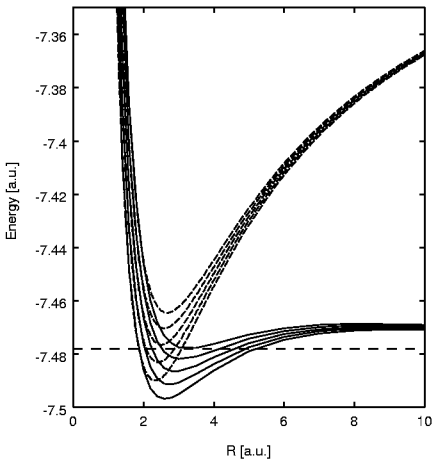

Figure 3: Adiabatic potentials for $\bar{p} + \mathrm{Li}$ and $\bar{p} + \mathrm{Li}^+$ with $62 \leq L \leq 66$. The dot lines indicates the energy level of the rested $\bar{p}$ and the ground state of Li atom in the limit as $R \to \infty$.

Nonneutral Plasmas and Antihydrogen Production

Kevin Fine, CERN and UC San Diego

I will give a review of results from nonneutral plasma physics relevant to the production of antihydrogen. Traditionally, the nonneutral trap community has been divided into two separate groups: particle and atomic physicists who trap small numbers of particles in Penning traps with hyperbolic electrodes, and plasma physicists who trap large numbers of particles in cylindrical Malmberg-Penning traps. The dividing point between the two groups is the plasma criterion, *i.e.* the plasma regime begins at the point where the Debye length is less than the radius of the charge cloud. The Debye length is given by $\lambda_D = \sqrt{4\pi ne^2/kT}$, where n is the density of the charged particles and T is the particle temperature.

Both kinds of traps will be necessary for antihydrogen production. The antiproton clouds will have small numbers, using techniques developed by the first group. For effective recombination, the positron density should be large and the temperature low, pushing the positron cloud into the plasma regime.

I will review the ideas and techniques obtained over decades of experience with containing plasmas. In particular, I will discuss the loss of plasma containment due to external field errors, and the effect of this on plasma temperature. I will also discuss techniques to measure the plasma temperature, and to control the “diocotron” or off center mode, and the use of this mode as a diagnostic.

Status Report on the ASACUSA Antiproton Trapping System

T.Ichioka[A,B], H.Higaki[A], N.Oshima[B], M.Hori[C], K.Kuroki[D], A.Mohri[B], K.Komaki[A], Y.Yamazaki[A,B]

[A]Institute of Physics Univ. of Tokyo (Komaba), [B]RIKEN,
[C]Faculty of Science Univ. of Tokyo (Hongo),
[D]National Research Institute of Police Science

In ASACUSA project, experiments are planned to investigate initial formation processes of antiprotonic atoms, interaction between antimatter and matter etc., most of which require ultra-low energy antiproton beams. In our scheme, MeV-energy antiprotons from AD will have several tens of keV after passing through an RFQ, post decelerator. Those antiprotons enter into a Multi-ring harmonic trap described below and the well-known electron cooling technique will be applied. Cold antiprotons, together with electrons, are supposed to behave as a nonneutral plasma.

In designing the trap, following two points are considered :

1. Extraction of antiprotons from the trap which is located in the strong magnetic field.

   As they tend to follow the field line, it is essential to axialize the particles for their extraction as a beam. One of the electrodes is azimuthally segmented for the radial compression of the plasma.

2. Reasonable cooling of 10^{6-7} antiprotons within one minute (the value of which comes from the pulse interval at AD).

   Harmonic potential is used to ensure the longer trapping time. By applying rotational electric field, plasma shape will become prolate and its density will become larger. To reduce the space potential, central harmonic region is elongated to 10cm in the axial direction. Multi-ring structure* † is exploited to generate such a harmonic potential.

Test experiments are being performed with protons($\sim$50keV) and H^- ions($\sim$1keV) from Duoplasmatron ion source. Results will be presented.

---

* H.Higaki and A.Mohri, Jpn.J.Appl.Phys. **36**(1997), 5300–5305

† A.Mohri *et al.* Jpn.J.Appl.Phys. **37**(1998), 664–670

Two-Component Nonequilibrium Nonneutral Plasma in Penning-Malmberg Trap

Hiroo Totsuji,[1] Kenji Tsuruta, Chieko Totsuji, Koichi Nakano, Kenichi Kamon, Tokunari Kishimoto

Faculty of Engineering, Okayama University
Tsushimanaka 3-1-1, Okayama 700-8530, Japan

Introduction

The Penning-Malmberg trap has been widely applied to precision measurements and analyses of properties of plasma bulk.[1] The assembly of trapped charged particles can be also used to host other particles introduced into the trap. The cooling of high energy particles by cryogenic plasmas in the trap may be one of typical examples of such applications.[2] In these applications, the behavior of multicomponent plasmas in the trap is of essential importance. The purpose of this article is to analyze the thermal equlibrium and relaxation processes in multicomponent plasmas in the Penning-Malmberg trap.

We consider the Penning-Malmberg trap with the magnetic field in the z-direction $\mathbf{B} = B\hat{z}$. For simplicity, we assume the cylindrical symmetry around the z-axis and denote the coordinates of particles $\mathbf{r}$ as (R, θ, z).

In thermal equilibrium, trapped particles perform a solid rotation around the z-axis. The Hamiltonian in the coordinate frame rotating with ω is given by $H = H_0 - \omega M_z$, where M_z is the z-component of total canonical angular momentum, and rewritten into the form[3]

$$H = H_0' + \frac{1}{2}\sum_i k_i R_i^2, \qquad (1)$$

where

$$\frac{1}{2}\sum_i k_i R_i^2 = -\frac{1}{2}\omega\sum_i (q_i B + m_i\omega) R_i^2, \qquad (2)$$

and H_0' has the same form as the Hamiltonian for particles in the rest frame. The term (2) in H serves as a potential which confines particles around the z-axis. The canonical distribution in the rotating frame is thus given by that of a system where particles are in the external potential $\sum_i U_{ext}(R_i) + \frac{1}{2}\sum_i k_i R_i^2$ and are mutually interacting via the potential $U_{int}(\{\mathbf{r}_i\})$.[4]

When we have several species of charged particles in the trap, the confining potential for the species α is given by $\frac{1}{2}k_\alpha R^2$, where

$$k_\alpha = -\omega(q_\alpha B + m_\alpha\omega). \qquad (3)$$

For electrons and antiprotons, $q_\alpha = -e < 0$, and the Hamiltonian in the rotation frame is given by

$$H = H_0' + \frac{1}{2}\omega \sum_{electrons} (eB - m_e\omega) R_i^2 + \frac{1}{2}\omega \sum_{antiprotons} (eB - m_p\omega) R_i^2. \qquad (4)$$

For confinement of both species of particles, $\omega > 0$, and it is also necessary to have $\omega(eB - m_p\omega) > 0$.

Parameters

Here we list typical values of paramters expected in experiments to cool antiprotons by cryogenic electrons trapped in the Penning-Malmberg trap.

magnetic field	B	5T
trap length		1cm
trap radius		0.1cm
electron density	n_e	10^9cm^{-3}
antiproton density	n_p	10^7cm^{-3}
electron temperature	T_e	10K
antiproton temperature	T_p	$> 10^4$K
electron solid rotation	ω_e	10^5s^{-1}

[1]E-mail: totsuji@elec.okayama-u.ac.jp

electron cyclotron frequency	eB/m_e	$9 \cdot 10^{11}\mathrm{s}^{-1}$
antiproton cyclotron frequency	eB/m_p	$5 \cdot 10^{8}\mathrm{s}^{-1}$

electron Debye length	$(\varepsilon_0 k_B T_e/n_e e^2)^{1/2}$	$7 \cdot 10^{-4}$cm
antiproton Debye length	$(\varepsilon_0 k_B T_p/n_p e^2)^{1/2}$	$2 \cdot 10^{-1}$cm
electron mean distance	$(3/4\pi n_e)^{1/3}$	$6 \cdot 10^{-4}$cm
antiproton mean distance	$(3/4\pi n_p)^{1/3}$	$3 \cdot 10^{-3}$cm
electron cyclotron radius	$2\pi v_{th,e}/(eB/m_e)$	$9 \cdot 10^{-6}$cm
antiproton cyclotron radius	$2\pi v_{th,p}/(eB/m_p)$	$1 \cdot 10^{-2}$cm
close collision radius	$e^2/4\pi\varepsilon_0 k_B T$	$2 \cdot 10^{-4}$cm

The Coulomb coupling constants are given by

Γ_e (electrons)	$e^2/4\pi\varepsilon_0 a_e k_B T$	$3 \cdot 10^{-1}$
Γ_p (antiprotons)	$e^2/4\pi\varepsilon_0 a_p k_B T$	$6 \cdot 10^{-5}$

We have an inequality for length scales

$$\text{electron cyclotron radius} \ll \text{electron mean distance} \ll \text{antiproton mean distance} \ll \text{antiproton cyclotron radius.} \tag{5}$$

Equilibrium Distribution

The distribution in thermal equilibrium is determined by the frequency of solid rotation and the temperature: For centrifugal separation, the fast rotation and/or the strong Coulomb coupling are necessary. Examples of the results of small scale molecular dynamics simulations are shown in figures. We expect no centrifugal separations for parameters 10 times smaller than these values. Results of large scale simulations will also be presented.

Relaxation Processes

Let us now consider the relaxation processes which occur when energetic antiprotons are introduced into cryogenic electrons.

When antiprotons are impinging cold electrons with the velocity $v_{p\|}$, the loss rate of parallel energy is estimated by moving to the frame where the antiproton is at rest and the electron is coming with the velocity $-v_{p\|}$ from $z = \infty$. In the strong magnetic field, the drift approximation may be applied.[5] In this approximation, electrons within the impact parameter

$$e^2/4\pi\varepsilon_0(m_e/2)v_{p\|}^2 \tag{6}$$

are reflected and those with the impact parameter larger than the above make a drift motion around the antiproton and eventually move to $z = -\infty$. The perpendicular energy $E_\perp$ is an

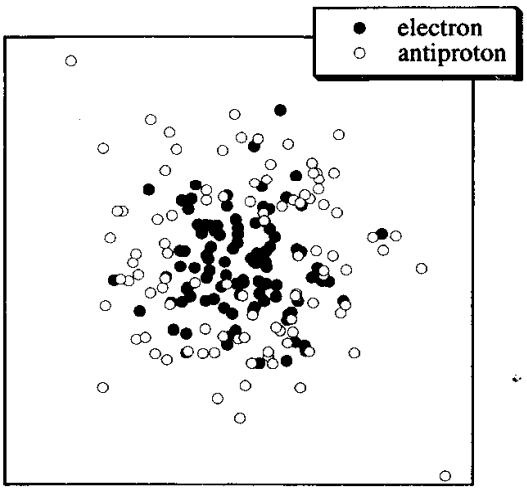

$\omega_c/(eBm_e)=3*10^{-4}$, Γ=0.2

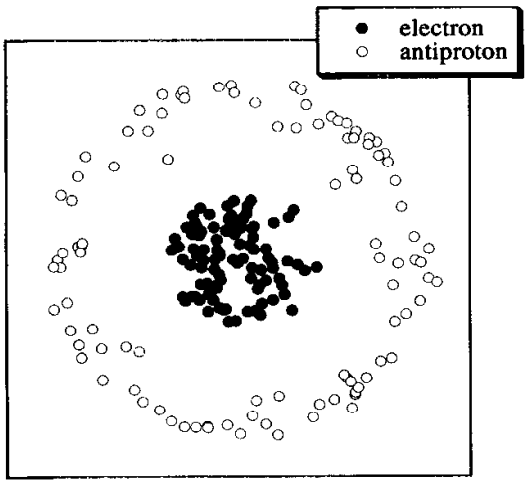

$\omega_c/(eBm_e)=3*10^{-4}$, $\Gamma=15$

adiabatic invariant.

Estimating the frequency of collisions with the impact parameter smaller than (6), we have

$$\frac{d}{dt}E_{p\|} = -\frac{1}{\tau_1}E_{p\|}, \tag{7}$$

where

$$\frac{1}{\tau_1} = 2^{5/2}\pi n_e \left(\frac{e^2}{4\pi\varepsilon_0}\right)^2 \frac{1}{m_e^{1/2}E_{p\|}^{3/2}} \left(\frac{m_p}{m_e}\right)^{1/2}. \tag{8}$$

For $n_e = 10^9 cm^{-3}, E_{p\|} = 10^4 K$,

$$\frac{1}{\tau_1} \sim 7 \cdot 10^5 s^{-1}. \tag{9}$$

In strong magnetic field where cyclotron radius is smaller than the close collision radius, parallel and perpendicular components of energy of electrons relax separately to the Maxwell distributions with different temperatures: The relaxation between these components is a slow process limited by the many-body adiabatic invariance.[6, 7, 8] The relaxation time for the latter is written as

$$\frac{d}{dt}T_{e\|} = -\frac{1}{\tau_2}(T_{e\|} - T_{e\perp}), \tag{10}$$

$$\frac{1}{\tau_2} = n_e \left(\frac{2e^2}{4\pi\varepsilon_0 k_B T_{e\|}}\right)^2 \left(\frac{k_B T_{e\|}}{m_e/2}\right)^{1/2} I(\kappa), \tag{11}$$

where $I(\kappa)$ is a function of

$$\kappa = \frac{eB}{m_e}\frac{2e^2}{4\pi\varepsilon_0 k_B T_{e\|}}\left(\frac{k_B T_{e\|}}{m_e/2}\right)^{-1/2}. \tag{12}$$

For $n_e = 10^9 cm^{-3}, T_{e\|} \sim T_{e\perp} \sim 10K$, and $B = 5T$, $\kappa = 1.7 \cdot 10^2$ and $\tau_2^{-1} \sim 10^0 s^{-1}$.

We now fix the magnetic field at 5T and the density and the temperature of electrons at $10^9 \mathrm{cm}^{-3}$ and 10K, respectively. When $E_{p\|} > 10^8 K(10\mathrm{keV})$, $\tau_1 < \tau_2$ and the relaxation is limited by the process $E_{p\|} \to T_{e\|}$. When $E_{p\|} < 10^8 K(10\mathrm{keV})$, $\tau_1 > \tau_2$ and the relaxation is limited by the process $T_{e\|} \to T_{e\perp}$.

We will also discuss the results of molecular dynamics simulations on these relaxation processes.

References

[1] For example, T. B. Mitcell, J. J. Bollinger, D. H. E. Dubin, X.-P. Huang, W. M. Itano, and R. H. Baughman, Science **282**, 1290(1998).

[2] *Atomic Spectroscopy and Collisions Using Slow Antiprotons (ASACUSA)*, CERN/SPSC 97-19, CERN/SPSC P-307.

[3] L. D. Landau and E. M. Lifshitz, *Mechanics, Third Edition* (Pergamon, Oxford, 1976), §39.

[4] J. H. Malmberg and T. M. O'Neil, Phys. Rev. Lett., **39**, 1333(1977).

[5] E. M. Lifshitz and L. P. Pitaevskii, *Physical Kinetics* (Pergamon, Oxford, 1981), §60.

[6] T. M. O'Neil, Phys. Fluids, **26**, 2128(1983).

[7] T. M. O'Neil and P. G. Hjorth, Phys. Fluids, **28**, 3241(1985).

[8] M. E. Glinsky, T. M. O'Neil, M. N. Rosenbluth, K. Tsuruta, and S. Ichimaru, Phys. Fluids B, **4**, 1156(1992).

High precision, two-photon spectroscopy of antiprotonic helium atoms and other experiments using ultra-low density targets

M. Hori
Department of Physics, School of Science, University of Tokyo

When antiprotons are stopped in a dense helium target, some 3% survive by forming metastable antiprotonic helium atoms ($\overline{p}$He). In the present talk, we describe future experiments that will be carried out using the new Antiproton Decelerator facility at CERN; we plan to measure the transition energies of this atom to an accuracy of 50 ppb, which is a tenfold improvement in accuracy over previous experiments. By comparing this data with high-precision three-body calculations, we may be able to improve the known value of the antiprotonic Rydberg constant.

Now our experimental precision is limited by several factors, which present technical challenges which will be formidable to overcome. First, the $\overline{p}$He atom must be produced in an ultra low-density helium target (with a pressure of $P = 1$ mbar and temperature of $T = 5$ K) to decrease the effects of collisional broadening and shifting of the resonance lines. This requires a mono-energetic antiproton beam with an energy of around $T = 0.1$ MeV, nearly two orders of magnitude lower in energy than the beams which are currently available; a new radio-frequency quadrapole post-decelerator is now being constructed at CERN to provide such a high-quality beam.

Secondly, a new high-power laser system, based on pulsed amplification of a stabilized CW-ring laser, will be developed to obtain a laser beam with a bandwidth of ~ 50 MHz. The laser must be specially designed to ignite in precise synchronization with the arrival of the pulsed antiproton beam at the helium target, while maintaining a narrow bandwidth and stable output energy over long periods of time.

Thirdly, a Doppler-free, two-photon spectroscopy technique using two counter-propagating laser beams must be used, to cancel the Doppler broadening of the resonance lines caused by the thermal motion of the atom. Calculations show that the transition $\Delta n = 2$, $\Delta \ell = 2$ (n and ℓ being the principal quantum number and orbital angular momentum quantum number of the $\overline{p}\mathrm{He}^+$ state, respectively) is especially suitable in terms of the expected signal-to-noise ratio and the necessary laser energy.

Non-Adiabatic High-Precision Calculation of Antiprotonic Helium Atomcule and Determination of Antiproton Mass

Yasushi Kino,[1] Masayasu Kamimura [2] and Hiroshi Kudo [1]

[1] *Department of Chemistry, Tohoku University, Sendai 980-8578, Japan*
[2] *Department of Physics, Kyushu University, Fukuoka 812-8581, Japan*

The metastable states of antiprotonic helium "atomcule" (= *atom+molecule*) are one of the powerful systems to study the basic properties of antiparticle systems, because they only have extremely long lifetimes ($\sim \mu$s) in the normal matter. We calculated the energy levels of the metastable states of exotic Coulomb-three-body systems $\bar{\mathrm{p}}\mathrm{He}^+ (=\mathrm{He}^{2+} + e^- + \bar{\mathrm{p}})$ having large interacting angular momenta of 30–40 with the non-adiabatic coupled rearrangement channel method using Gaussian basis functions [1]. The calculated energies are agree well with the latest calculation [2]. In Table 1, an excellent agreement between theory and experiment are shown. And the discrepancies between them were within the experimental error.

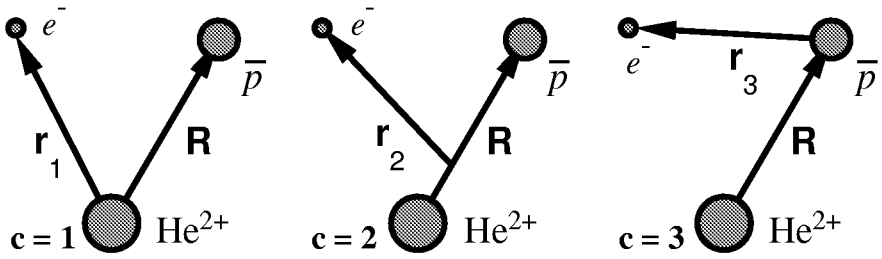

Figure 1: Three rearrangement channels.

The total wave function is described with a sum of the amplitudes of three rearrangement channels c=1–3 of Figure 1:

$$\Psi_{vJM} = \sum_{c=1}^{3} \sum_{n,N} \sum_{\ell_c, L_c} A_{v,n\ell_c N L_c}\, r_c^{\ell_c} R^{L_c}\, \mathrm{e}^{-\left(\frac{r_c}{r_n}\right)^2 - \left(\frac{R}{R_N}\right)^2} [Y_{\ell_c}(\hat{\mathbf{r}}_c) \otimes Y_{L_c}(\hat{\mathbf{R}})]_{JM}. \qquad (1)$$

Channel c=1 is suited for describing the atomic picture. Channel c=2 is for describing the diatomic molecular picture. Channel c=3 is for describing the strong correlation between the electron and the antiproton. The Gaussian ranges are taken to be geometrical progression. The relativistic and QED corrections were calculated, which reduced the discrepancy between the theory and the experiment by 50 ppm.

Table 1: The transition wavelengths and the uncertainty of antiproton mass Δx.

Transition	Calculated wavelength (nm)	Observed wavelength (nm)	Δx
(35,3)-(34,3)	597.2573 [4]	597.2570 ± 0.0003 [5]	1×10^{-7}
(34,2)-(33,2)	470.7220 [4]	470.7220 ± 0.0006 [5]	3×10^{-7}

We assumed that the antiproton mass was equal to the proton. The measured charge-to-mass ratio of antiproton is equal to the proton with 10^{-10} uncertainty [6], but the antiproton mass and charge were not measured individually with such high accuracy. The antiproton mass was estimated with 2×10^{-5} uncertainty using the X-ray measurement of antiprotonic atoms [7]. The transition wavelengths (energies) show the different dependence of mass and charge from the charge-to-mass ratio. To estimate the uncertainty of antiproton mass from the experimental data, we therefore recalculated the wavelength using the antiproton mass scaled with $1+\Delta x$ against the proton mass, $m_{\bar{p}} = (1+\Delta x)m_p$. The antiproton charge was also scaled to keep the charge-to-mass ratio, $e_{\bar{p}} = (1+\Delta x)e_p$. We recalculated the transition wavelengths as a function of asymmetric parameter Δx. The uncertainty Δx is estimated using the uncertainty of the experimental wavelengths $\Delta\lambda_{\rm expt}$.

$$\Delta x = \frac{\Delta m_{\bar{p}}}{m_p} = \Delta\lambda_{\rm expt}\left(\frac{d\lambda}{dx}\right)^{-1}_{\rm cal} \tag{2}$$

$(d\lambda/dx)_{\rm cal}$ is obtained by the slope of Figure 2. The last column of the Table 1 shows that this work reduced the uncertainty of antiproton mass by two orders of magnitude. We also calculated the Δx dependence of the energies of the subsystem to investigate the structure and the dynamics of the atomcules.

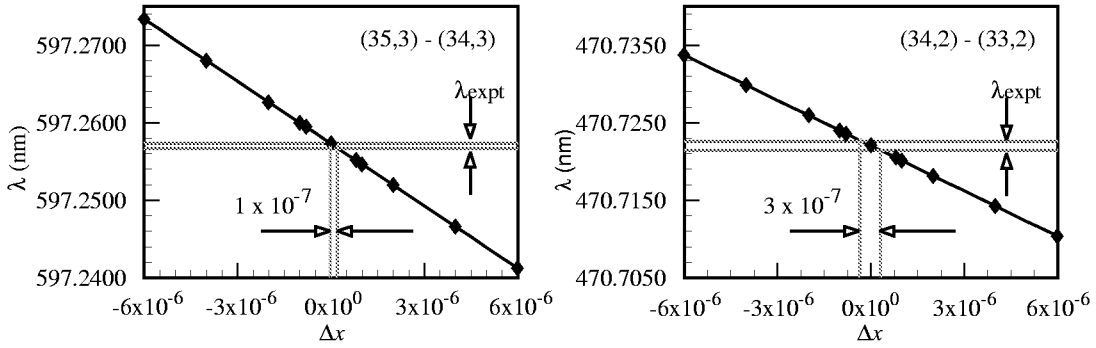

Figure 2: The calculated wavelengths as a function of asymmetric parameter Δx. Here closed diamonds shows the calculated values and solid line is the guide for the eyes.

References

[1] M. Kamimura, Phys. Rev. A**38** (1988) 621.
[2] V.I. Korobov, Hyperfine Interactions, *in print.*
[3] V.I. Korobov, D. Bakalov and H.J. Monkhorst, Phys. Rev. A**59** (1999) R919.
[4] Y. Kino, M. Kamimura and H. Kudo, Hyperfine Interactions, *in print.*
[5] H.A. Torii *et al.*, Phys. Rev. A**59** (1999) 223.
[6] G. Gabrielse *et al.*, Phys. Rev. Lett. **82** (1999) 3198.
[7] P. Roberson *et al.*, Phys. Rev. C**16** (1977) 1945.

Spectroscopy of the antiprotonic atomcule

V.I. Korobov

Joint Institute for Nuclear Research
141980, Dubna, Russia

In this talk we discuss calculation of the α^2 (au) and α^4 relativistic corrections for the bound electron and α^2 corrections for the heavy nuclei as well as the one and two loop QED corrections such as the electron self-energy and vacuum polarization up to the order of $\alpha^5 \ln \alpha$.

Eventually after inclusion of the higher order radiative corrections which do not require significant computational efforts we anticipate to improve theoretical prediction for the transition energies to the level of a few ppb!

The other topic which is suggested to discuss is the dynamics of the population of fine and hyperfine sublevels of a metastable state under *ac* and *dc* magnetic fields.

Nuclear absorption process in antiprotonic helium atoms

T. Koike and Y. Akaishi
High Energy Accelerator Research Organization, Tanashi Branch, Tanashi, Japan

The antiproton in matter forms the highly-excited antiprotonic atom, and then cascade down to lower orbit by various de-excitation processes, and finally absorbed into nuclei by strong interaction. In nuclear physics, we often encounter the following problem: From which atomic orbit is antiproton absorbed into the nucleus by strong interaction? In the case of helium atom, the Stark-mixing process makes high-ns state absorption increase. However, we have not yet come to quantitative answer for the ratio of s-orbit absorption rate vs. p-orbit one.

Our purpose is to get a reliable answer for the the s- and p-orbit absorption ratio of antiprotonic helium atoms. To do this, we construct a new cascade-model [1]. Our cascade calculation begins from such states that ionized $\bar{p}$-α is formed. Processes included in our cascade calculation are the followings;

1. Radiative transition: $(\bar{p}\alpha)_i \rightarrow (\bar{p}\alpha)_f + \gamma$

2. External Auger transition: $(\bar{p}\alpha)_i + {}^4\mathrm{He} \rightarrow (\bar{p}\alpha)_f + {}^4\mathrm{He}^+ + e^-$

3. Molecular ion formation and subsequent Auger transition
   ${}^4\mathrm{He} + {}^4\mathrm{He} + (\bar{p}\alpha)_i \rightarrow {}^4\mathrm{He} + [{}^4\mathrm{He}\text{-}(\bar{p}\alpha)_i]^+, \qquad [{}^4\mathrm{He}\text{-}(\bar{p}\alpha)_i]^+ \rightarrow (\bar{p}\alpha)_f + {}^4\mathrm{He}^+ + e^-$

4. Stark-mixing process: $(\bar{p}\alpha)_i + {}^4\mathrm{He} \rightarrow (\bar{p}\alpha)_f + {}^4\mathrm{He}, \quad n_i = n_f$

5. Elastic Scattering: $(\bar{p}\alpha)_i + {}^4\mathrm{He} \rightarrow (\bar{p}\alpha)_i + {}^4\mathrm{He}$

6. Nuclear absorption by strong interaction

We compare the results of the cascade calculation using two different model for Stark-mixing process. One is our new model based on the impact parameter method [1]. Other is the phenomenological model used so far, which is often called as "siding transition" [2]. We show that both of two models can well reproduce the experimental x-ray yields observed at low-n states, but they give considerably different s- and p-orbit absorption rate at high-n state.

[1] T. Koike, Ph.D.Thesis, Hokkaido University (1998);
T. Koike and Y. Akaishi, Nucl. Phys. **A639** (1998) 521c.
[2] C. A. Baker *et al.*, Nucl. Phys. **A494**, 507 (1989).

Collisions of Antiprotonic Atomcules with He Atoms

Grigori Korenman

Institute of Nuclear Physics, Moscow State University, 119899 Moscow, Russia

Experimental discovery and high precision studies of antiprotonic helium metastable states pose many theoretical problems on $\bar{p}He^+$ "atomcule" interaction with ordinary atoms and molecules. We discuss elastic and inelastic collisions of the atomcule with He atoms using the effective potential operator [1], which includes scalar and tensor terms and has a form of Van der Waals attraction at large distance and soft repulsion at small R,

$$\hat{V}(\mathbf{R}) = -[C_6 + G_6 P_2(\cos\theta)](R^2 - r_c^2)/(R^2 + r_0^2)^4, \qquad (1)$$

where θ is the angle between $\mathbf{R}$ and the quantization axis. The values of C_6 and G_6 are, in fact, matrixes on atomcule quantum numbers (n, L) and, for a large n, $C_6 \simeq \alpha\langle\mathbf{D}^2\rangle$, $G_6 \simeq \alpha\langle\mathbf{D}^2 P_2(\cos\theta_D)\rangle$, where α is a polarizability of He atom and $\mathbf{D}$ is the atomcule dipole operator.

Quantum scattering phases $\delta_l(E)$ for the potential (**??**) with reasonable values of the parameters show the S-, P-, and D-wave resonances at very low energy ($E \sim 2 \div 6$ K) and (weakly) bound S- and P-states. With the potential (1) we calculate elastic and transport cross sections, and consider a competition between collisional quenching of "hot" atomcule [2] and their thermalization.

A specific behaviour of the phase differences ($\delta_l^i - \delta_l^f$) allows to explain the data on density shifts Δ and broadenings γ of atomcule E1-spectral lines ($i \to f$) at low temperature, including an unusual relation $\Delta \gg \gamma$. With the parameters $C_6^i = 2.82$, $C_6^f = 2.68$, $r_0 = 2.8$, $r_c = 3.0$ a.u. we obtain $\Delta/N = 4.25$, $\gamma/N = 0.36$ (in units of 10^{-3} a.u.) at T=6 K for the transition 39,35 $\to$ 38,34, whereas the experimental values are 4.15±0.07 and 0.34±0.13, respectively.

Due to tensor term in the potential, the collisions $(\bar{p}He^+) - He$ can produce (i) transitions between HFS sublevels $F_- = L - 1/2 \leftrightarrow F_+ = L + 1/2$ and a relaxation of the sublevel populations, and (ii) shift and broadening of the spectral line for radiative M1-transition $F_- \to F_+$. We found that the first effect is rather small, because the non-diagonal matrix element is proportional to $1/L^2$, and the rate of relaxation is estimated of order $10^3 \div 10^4\, s^{-1}$ at the density $10^{20}\, cm^{-3}$. On the other hand, the difference between the diagonal matrix elements of the tensor interaction for F_- and F_+ is of the same order of value (1/L) as the difference of the diagonal matrix elements of scalar interaction for the states nL and n-1,L-1. With account for a numerical factor, the shift of the spectral line $F_- \to F_+$ may be of order 0.1 - 0.01 of shift for the spectral line $nL \to n-1,\, L-1$.

References

[1] G.Ya.Korenman, Hyperfine Interactions, (1999), to be published.
[2] G.Ya.Korenman, Hyperfine Interactions, **103**, 341 (1996).

Density shift and broadening of the transition lines in antiprotonic helium

D.Bakalov, B.Jeziorski, T.Korona, K.Szalewicz and E.Tchukova

The density shift and broadening of the transition lines from metastable states of antiprotonic helium atoms is being studied on the ground of an interaction potential calculated ab initio within the frame of symmetry-adapted perturbation theory.

Does a solvated antiproton exist?

Toshiyuki Azuma
Institute of Applied Physics, University of Tsukuba,
Tsukuba, Ibaraki, 305-8573, JAPAN

Recently the behavior of anti-proton in liquid He has been extensively investigated, while a few information is so far available for other liquids. Here we try to evaluate the possibility of finding a solvated state in liquid phase by comparison of anti-proton with other particles.

The existence of solvated states of excess electrons in water has been well known since early 1960's. And an ammoniated electron precedes it. It is generally believed that solvated electron is localized within a small cavity region around which several water molecules are coordinated (although the excess electron may, to some extent, be delocalized onto molecules). The stability of the ground state is primarily due to electrostatic interaction with dipoles of surrounding molecules. Theoretically various models ranging from the potential well model to the cluster model, which has developed to recent *ab initio* molecular orbital calculations, have been proposed. In the case of excess electrons in non-polar liquids like He, Ne and H_2, they produce bubble states. The origin of the bubble states is repelling of electron by the electrons in the surrounding molecules/atoms because of the Coulomb forces and the exchange effect. The latter is a consequence of the Pauli principle, which states that two or more electrons cannot occupy the same state.

Concerning to positron, solvated positron is naturally considered to exist. For examples, at increasing density the lifetime of a free positron decreases to that of liquid NH_3 in gaseous NH_3 at room temperature (RT) already at density of ~0.25% of the liquid density. This is supposed to indicate positron annihilation from the solvated positron state in a cluster of NH_3. On the other hand positronium (Ps) forms the bubble states in many kinds of liquids. It is an electron constituting Ps which acts as the origin of bubble, and is repelled by the electrons in the molecules/atoms.

For positive/negative muon, i.e., heavier hadron particles, solvated states have not been reported yet, possibly because of its difficulty in identification. Muonium (Mu) is observed in various liquids except in liquid He or Ne due to the larger ionization

energy compared with Mu binding energy, and no information on the bubble states has been reported.

Solvated proton in polar liquids is a well-discussed idea. A variety of theoretical calculations of the cluster model have been reported.

Here some key points to consider the bubble state of antiproton are,

1) Pauli principle responsible for the bubble states does not work for anti-proton in contrast with electron.

2) The bubble state is naively considered to be produced when an internal pressure on the bubble wall created by the zero-point kinetic motion of electron or Ps, balances the pressure generated by the surface tension of the liquid and the external pressure.

Thereby lower zero point energy for a heavier hadron particle lead to instability of the bubble state.

Furthermore a key point for the solvated state of antiproton is,

1) During energy loss process, anti-proton once captured by a host atom quickly decays from the excited states, captured by nucleus and annihilates into pions etc. The cascade time is largely shortened by the Stark mixing by the surrounding atom/molecule in liquids. On the other hand the solvated state requires “thermalized” or “almost-thermalized” anti-proton. The required time for forming solvated electrons in water at RT is reported to be of the order of sub-ps. It is of question whether anti-proton survives until its solvation accomplishes.

Taking the above points into consideration we will discuss the possibility of the solvated/bubble states of anti-proton and experimental clues to identify them in detail.

Comparison of multi-differential ionization cross sections in fast antiproton and proton on Helium collisions --- A proposal for future studies with a table sized PBAR-storage ring

H.Schmidt-Böcking University Frankfurt, Frankfurt/FRG et al. (Frankfurt-Aarhus-Freiburg-GSI-CERN-Collaboration)

Doubly differential electron emission cross sections as function of the longitudinal momenta of electron and recoil ion have been measured for single ionization in fast pbar on He collisions. In this contribution the data will be discussed with respect to different calculations. Within the experimental uncertainty these data agree with those for proton impact, but do not agree within the error bars with theory. For proton on He also data for the different double ionization channels will be presented and anomalies in the kinematics will be discussed.

For future systematics experimental studies of highly differential ionzation cross sections of pbar on atoms and molecules collisions the installation of a table sized electrostatic storage ring (nearly identical with the ELISA ring in Aarhus) at the pbar decelleration facilty at CERN is discussed.

Ionization of H and He atoms by antiprotons revisited

C. D. Lin, Tech Lee, Clara Illescas and Emil Sidky
Department of Physics, Kansas State University
Manhattan, KS 66506 USA

The ionization cross sections of H and He targets by antiprotons are revisited. We used different theoretical models to perform calculations, including coupled channel method, the direct numerical integration of the time-dependent Schrodinger equation method and the classical trajectory Monte Carlo method to obtain the total ionization cross sections. We conclude that the existing experimental ionization data for He target at low energies are probably questionable. We also calculated the ejected electron momentum distributions and compared the results for collisions by protons.

One of the earliest atomic collision experiments involving antiproton beams is the measurement of ionization cross sections of He and other gases, and later the atomic hydrogen targets. While there have been many discussions on the ratios of cross sections for double ionization to single ionization on He targets, in this talk I will focus on the problems in the lower energy region, in anticipation of the new low energy antiproton beams that are to become available again in the coming years.

Collisions of antiprotons with atomic hydrogen at low energies are of interest in that it is one of the most elementary three-body collision systems, and by comparing the results with collisions of protons with atomic hydrogen, one can assess in what way the role of the charge of the projectile plays in processes such as the ionization. It is expected that the ionization cross sections for these two projectiles to be identical in the high energy limit. This will be the case when the first Born approximation can be used to describe the ionization process. On the other hand, it is not clear at what energies the Born approximation will become valid.

The mechanism for ionization by protons or by antiprotons at low energies are much less clear and there are no well established theoretical models. Experimental data for collision energies below 10 keV or so are rare for both projectiles. For protons the difficulty lies in the small ionization cross sections, and for antiprotons the difficulty so far mostly is the lack of intense beams in this energy range. On the theoretical side, ionization is a rare process in proton-hydrogen collisions at low energies and currently the main question is what is the role of the so-called “saddle-point mechanism” for ionization. For antiproton collisions there is no saddle point mechanism and the ionization cross sections actually do not drop rapidly as the collision energy is reduced, as in the proton case. The different theoretical calculations for the total ionization cross sections for antiprotons on atomic hydrogen appear to all agree in the 1-25 keV region now. In anticipating of the possible experimental measurements of the electron spectra we have calculated the ejected momentum distributions in the longitudinal and the transverse directions, and compared to the similar spectra for proton impact. The significance of the Fermi-Teller limit will also be addressed.

For collisional ionization of He by antiprotons, the cross sections have been determined for collision energies down to about 15 keV [1] in an early experiment. However, the experimental results are in disagreement with most of the theoretical calculations. For this two-electron system, the theoretical calculations employed more approximations, in particular, the role of electron-electron interaction is often treated inadequately. We have employed two different models to perform the calculations for this case and obtained cross sections which are significantly different from the experimental data for energies below 40 keV. Based on this result and also the expected slower energy dependence for ionization cross sections by antiprotons at low energies (as seen in H target) we suggested that the total ionization cross sections for He target be remeasured again.

Reference

1. P. Hvelplund et al, J. Phys. **B27**, 925 (1994).

Post collision interaction at proton, antiproton - atom collision

Akos Kover

Institute of Nuclear Research of Hung. Acad. Sci. (ATOMKI)
Debrecen, POB 51, H-4001, Hungary

The investigation of the energy and angular distribution of electron spectra ejected from ionising collisions provide more detailed information on the collision process especially when it is combined with the variation of the sign of the projectile charge. The best candidates for this study are the proton - antiproton and electron - positron projectile pairs.

According to the first order theories the proton and antiproton impact on free atoms should provide the same ejected electron spectra. The experimental results for proton impact, however, indicate that higher order theories are necessary to describe the collision process, because a sharp (cusp) peak was found in the electron spectrum at a velocity close to that of the scattered projectile [1]. This enhancement can be explained as a final state interaction between the ionised electron and the outgoing projectile. Due to the attractive potential the ionised electron is captured to the projectile low-lying continuum states. It was called Electron Capture to the Continuum (ECC). Similar cusp peak was found at positron impact in the triple differential electron spectrum, too [2].

For negative charged projectiles an anticusp (a dip in the electron spectrum) is expected due to the repulsive potential. However, Yamazaki and co-workers have not found any dip in the convoy electron spectrum at antiproton impact using carbon foil [3]. They explained this results as the contribution of a dip-filling process due to phase-space uncorrelated electrons is very important. For electron impact on He, Guan-yan *et. al.* [4] published a deep minimum in the electron spectrum where the velocity of the two outgoing electrons is nearly the same indicating the importance of the final state interaction.

As it is seen experimental study has not been carried out for antiproton – free atom collision where the single collision condition is fulfilled. This lecture presents the calculated electron spectra ejected from antiproton – Ar collisions and suggests experimental methods to determine the anticusp at different ejection angles.

This work is supported by the Hungarian Scientific Research Found (OTKA No. T16636 and T025325)

References:

[1] G. B. Crooks and M. E. Rudd, Phys. Rev. Lett. **25** (1970) 1599.

[2] Á. Kövér and G. Laricchia, Phys. Rev. Lett. **80** (1998) 5309.

[3] Y. Yamazaki, Nucl. Instrum. Meth. in Phys. Res. B **96** (1995) 517.

[4] P. Guang-yan, P. Hvelplund, H. Knudsen, Y. Yamazaki, M. Brauner and J. S. Briggs, Phys. Rev. **47** (1993) 1531.

An Accurate Measurement of the p mass Using Highly Charged Ions in a Penning Trap

C. Carlberg, I. Bergström, H. Borgenstrand, T. Fritioff, G. Rouleau, J. Schoenfelder[†], and R. Schuch,

Atomic Physics, Stockholm University, Frescativ. 24, S-104 05 Stockholm, Sweden
([†]) GSI, Planckstr. 1, D64291 Darmstadt, Germany

The precision of mass measurements in a Penning trap increases linearly with the charge of the ion. Therefore, we have set up a Penning trap, named SMILEtrap, at the electron beam ion source of Manne Siegbahn Laboratory in Stockholm[1]. It produces bare nuclei up to charge 18 and charge states up to 65 for heavier elements. These externally produced highly charged ions are decelerated and injected into the trap and excited with their cyclotron frequencies. The time-of-flight method was applied for identification of the cyclotron resonances. The highly charged ions in different charge states served in the first place to verify the accuracy of the SMILEtrap mass spectrometer[2]. It was shown that the results for H_2^+, N^{6+}, $Ne^{9+,10+}$, $Si^{12+,13+,14+}$, and $Ar^{14+,16+}$, all agree within the statistical errors (0.3 - 1 ppb) within themselves and previously determined values. An analysis estimating the contribution from individual systematic errors does not allow a systematic error larger then +- 0.85 ppb[3].

The proton mass could be determined from mass doublet or almost doublet measurements by comparing the cyclotron frequencies of H_2^+ and heavy ions in high charge states: $C^{5+,6+}$, N^{6+}, $N^{7+,8+}$, $Ne^{9+,10+}$, $Si^{12+,13+,14+}$, and $Ar^{14+,16+}$. From these measurements a value of the proton mass with a weighted statistical error of +-0.16 ppb and an estimated systematic error of +-0.5 ppb is obtained[4].

References:

[1] C. Carlberg, H. Borgenstrand, G. Rouleau, R. Schuch, F. Söderberg, I. Bergström, R. Jertz, T. Schwartz, J. Stein, G. Bollen, H.J. Kluge, and R. Mann, Physica Scripta T59, 196, (1995)
[2] C. Carlberg, I. Bergström, H. Borgenstrand, T. Johansson, G. Rouleau, R. Schuch, J. Stein, and U. Surkau, Phys. Scr. Vol. T73, 347 (1997)
[3] C. Carlberg, Hyperfine Interactions 114, 177, (1998)
[4] C. Carlberg, I. Bergström, G. Bollen, H. Borgenstrand, T. Fritioff, R. Jertz, H.J. Kluge, L. Liljeby, G. Rouleau, R. Schuch, T. Schwartz,J. Schoenfelder, and F. Söderberg, NIM, to be publ.

A NEW LOW ENERGETIC MUON BEAM AND ITS APPLICATIONS

E. Morenzoni

Paul Scherrer Institut, CH-5232 Villigen PSI, Switzerland

The positive muon is an ideal projectile to study ion-solid and ion atom-interactions since it offers the simplicity of a heavy projectile with unit charge, such as the proton, but with a mass which is only about 1/9 of the latter. However, until now, studies of muon-solid collisions processes in the keV energy regime and below have been hampered by the lack of availability of monoenergetic muon beams. At PSI, in the last years, we have developed a tunable beam of low energetic (<30 keV) polarized positive muons. These muons are generated by moderating to epithermal energies an intense beam of ~ 4 MeV muons in an appropriate condensed gas layer. Besides allowing the use of muons as magnetic microprobes of thin films and surfaces, such a beam offers, from the point of view of the physics of atomic collisions, new interesting possibilities.

We will give an overview of the beam and of muon-solid collision experiments performed so far. Velocity scaling of energy loss, energy loss straggling and electron capture have been tested directly, by measuring simultaneously the interaction of muons and protons of equal velocity with thin carbon foils. By relaying on the specific behavior of polarized muons thermalizing in metals or insulators a new method has been developed that allows to obtain implantation profiles of low energetic muons in matter. We will show how, by measuring the slowing down and emission of a few eV muons from various materials, the interaction of eV muons in rare gas solids, ionic insulators and metals can be investigated and the different role played by elastic and electronic interactions (especially electron capture) elucidated. In particular the effects on the stopping power given by the presence of a minimum energy that can be transferred in electronic processes in insulators (threshold effect) can be shown.

CHANNELING OF SLOW ANTIPROTONS

N.M. Kabachnik[1], L.L. Balashova[2] and Ch. Trikalinos[3]

1 Faculty of Physics, University of Bielefeld, Bielefeld, Germany 2 Institute of Nuclear Physics, Moscow State University, Moscow, Russia 3 Physics Department, University of Athens, Athens, Greece

We have performed a Monte-Carlo simulation of penetration of slow (50-300 keV) antiprotons through Si single crystals along the main crystal axes. For the simulation we used a classical trajectory calculations within a string model with account of the position dependent energy loss, the energy straggling, the multiple scattering, and the thermal motion of the ions in the crystal. The influence of the crystaline structure on the energy spectrum and the angular distribution of scattered antiprotons is investigated. We show that the channeling effects are rather small in the energy spectrum leading to the small shift and widening of the spectra in comparison with a random direction. The angular distribution of antiprotons is strongly influenced by the crystal structure. The characteristic ring-shaped patterns ("doughnuts") are formed at least for thin crystals if the beam direction is slightly misaligned with the crystal axis direction. We investigated the projectile energy and the target thickness dependencies of the antiproton spectra and the angular distributions.

Tests of CPT, Lorentz Invariance and the WEP with Antihydrogen

Michael H. Holzscheiter
for the ATHENA Collaboration

Los Alamos National Laboratory
Physics Division, P-23, MS H803
Los Alamos, NM 87545, USA

Antihydrogen atoms, produced near rest, trapped in a magnetic well, and cooled to the lowest possible temperature (kinetic energy) could provide an extremely powerful tool for the search of violations of CPT and Lorentz invariance. Equally well, such a system could be used for searches of violations of the Weak Equivalence Principle (WEP) at high precision. We describe our plans to form a significant number of cold, trapped antihydrogen atoms for comparative precision spectroscopy of hydrogen and antihydrogen and comment on possible first experiments.

Making Hbar by Recombination in a Penning Trap

G. Andler, N. Eklöw, P. Glans, E Justiniano[†], E. Lindroth, and R. Schuch,

Atomic Physics, Stockholm University, Frescativ. 24, S-104 05 Stockholm, Sweden
([†]) Department of Physics, East Carolina University, Greenville, NC 27858, USA

In this contribution we discuss rates of forming antihydrogen (Hbar) atoms by recombination of antiprotons with positrons in a Penning trap. The estimates are based on mechanisms of radiative and three-body recombination, as well as observations of electron-ion recombination with the electron coolers of storage rings. Trapping parameters given in the ATHENA proposal are used. Considerations of this type are essential for finding optimum conditions for high recombination rates between antiprotons and positrons and, dependent on possible experimental requirements, enhanced recombination into certain quantum states of Hbar.

The systematic studies of recombination between free electrons and ions performed at electron coolers, have shown two phenomena of interest for this subject. One is the strongly enhanced rates as compared to theoretical descriptions of Radiative Recombination (RR), the other is the possibility of recombining into a certain quantum state of the atom by the presence of a laser field.

In the storage rings cooled ions collide with cold electrons. The collision energy is well controlled. In the ion-frame the electrons have a velocity spread corresponding to nowadays typically 1 meV in the transverse direction, relative to the ion velocity, and 0.1meV in the longitudinal direction. The electrons are guided by a weak longitudinal magnetic field of around 0.03 - 0.1 T. Surprisingly there is a consistent disagreement between recombination measurements in this environment and the rates obtained from the calculated cross section folded with the relevant temperatures[1,2].

Improvements of the electron beams in the coolers of the rings has constantly decreased the velocity spread in the transverse direction and the disagreement with theory has increased accordingly. The lowest electron temperature reached in a cooler is of the order of 10 K. The disagreement increases further with increasing nuclear charge[3]. The reason for the disagreement is not clear. One possible candidate is three-body recombination although many studies indicate that it cannot be efficient enough[4,5]. However, recent experimental results, one of which will be presented, indicate that a marked magnetic field dependence might exist.

In order to understand the influence of the magnetic field on recombination, in our group the radiative recombination of electrons being in a so called Landau states has been examined. It is the diamagnetic part of the Hamiltonian which give rise to the two-dimensional harmonic oscillatory potential in which the Landau states are bound. We have used a numerical procedure based on B-splines to calculate photoionization and then relate it to radiative recombination. It is quite clear that a B-field of 500 Gauss would be to weak for Landau states to be visible in this field range. Here, the classical results with zero magnetic field are well reproduced and then the predictions for a strong magnetic fields as used in a Penning trap are discussed.

It was demonstrated that recombination can be enhanced by factors of 100 by laser induced recombination [6,7]. Also here field effects were found to be important. They cause a laser induced recombination rate below the ionization threshold and it is shown

that this gain is sensitive on the orientation of the photons polarization vector relative to the field vector[8]. An additional unexplained laser induced recombination rate below the ionization threshold will be discussed. As a strong magnetic field, but also an electric space charge field, is present in a Penning trap, a good understanding of these effects is necessary.

References:

[1] Wolf A, Berger J, Bock M, Habs D, Hochadel B, Kilgus G, Neureither G, Schramm U, Schwalm D, Szmola E, Müller A, Wagner M and Schuch R 1991 ZP D **21** 69.
[2] Gao H, DeWitt D R, Schuch R, Zong W, Asp S, and Pajek M 1995 PRL **75** 4381
[3] Gao Hui, R. Schuch, E. Justiniano, D.R. DeWitt, W. Zong, W. Spies, and H. Lebius, Journ. Phys. B Lett. 30, L1, (1997).
[4] Pajek M and Schuch R 1997 *Hyperfine Interactions* **108** 185
[5] Zwicknagel G, Toepffer C and Reinhard P G 1996 *Hyperfine Interactions* **99** 285
[6] U. Schramm, J. Berger, M. Grieser, D. Habs, E. Jaeschke, G. Kilgus, D. Schwalm, A. Wolf, R. Neumann and R. Schuch, Phys. Rev. Lett. **67** (1991) 22
[7] S. Asp, R. Schuch, D.R. DeWitt, C. Biedermann, Gao Hui, W. Zong, G. Andler, and E. Justiniano, Nucl. Ins. Meth. B117, 31 (1996)
[8] E. Justiniano, G. Andler, P. Glans, W. Zong, M. Saito, and R. Schuch, American Institute of Physics, Woodbury, New York, 1999, in print.

Recombination of H-like ions with electrons: a testing ground for the formation of anti-hydrogen?

Stefan Schippers

Institut fuer Kernphysik, Strahlenzentrum der Justus-Liebig-Universitaet, Leihgesterner Weg 217, Giessen 35392, Germany

Abstract:

One possible path for the formation of anti-hydrogen may be radiative recombination (RR) of positrons with anti-protons. This talk summarizes today's knowledge about RR resulting from electron-ion collision studies performed at heavy ion storage rings. Special attention is given to the recombination at very low energies where a yet unexplained enhancement of the measured recombination rate over the theoretical prediction is observed. Detailed experimental studies of the dependence of this effect on various experimental parameters are presented.

HYDROGEN - ANTIHYDROGEN COLLISIONS

P. Froelich *, S. Jonsell * and A. Saenz ♯

*Department of Quantum Chemistry, Uppsala University, Box 518, 75120 Uppsala, Sweden
♯Max-Planck Institute for Quantum Optics, Hans-Kopfermann-Str. 1, D-85748 Garching, Germany

Matter - antimatter interaction is studied on the example of hydrogen - antihydrogen collisions. Cross sections for the rearrangement reaction resulting in formation of (excited) protonium and positronium in the final channel, according to $\mathrm{H} + \bar{\mathrm{H}} \rightarrow p\bar{p} + e^+e^-$, are calculated for the first time in the fully quantum mechanical approach. Implications on the experiments intending to trap and cool the antihydrogen are discussed.

In the present work we investigate the question of stability of antimatter in contact with matter. The primordial collisional interaction between hydrogen H and antihydrogen $\bar{\mathrm{H}}$ has been considered as the prototype reaction.

The recent advances in producing, trapping and cooling antiprotons and positrons opened the possibility of antihydrogen formation under experimental conditions.[1] This may allow the studies of antimatter and tests of fundamental physical principles such as charge - parity - time (CPT) invariance or the weak equivalence principle (WEP) for antiparticles. Such experiments are planned at CERN AD (Antiproton Decelerator) within the ASACUSA and ATHENA collaborations.[2]

To study the matter - antimatter interactions in general, and in particular to design and implement the experiments on trapping and cooling antihydrogen, the knowledge of the rates for elastic and inelastic atom - antiatom collisions is of paramount importance - but the previous treatments of the problem have been very scarce.[3,4]

The elastic cross section is responsible for cooling and the inelastic one, particularly the cross section for rearrangement resulting in formation of protonium, is responsible for losses of antihydrogen (*via* annihilation during the cascade in protonium).

In the present work we have focused interest on the rates for $p-\bar{p}$ and/or e^+-e^- annihilations during $\mathrm{H}-\bar{\mathrm{H}}$ collisions at low (down to ultra-cold) temperatures. In particular, we have calculated the (partial and total) rates for the collisional rearrangement reaction

$$\mathrm{H} + \bar{\mathrm{H}} \longrightarrow p\bar{p} + e^+e^- \qquad (1)$$

which inevitably leads to the annihilation of antiparticles from the bound states of protonium (pn $\equiv p\bar{p}$) and/or positronium (ps $\equiv e^+e^-$) formed in the final channel.

The cross section σ^{inel} for the formation of protonium - positronium pair through the above rearrangement collision has been calculated *for the first time by the fully quantum mechanical treatment* through computation of the scattering-theoretic transition matrix elements in the post-collisional approach. Born - Oppenheimer approximation has been invoked to obtain the scattering wave function in the initial channel, whereas the final channel wave functions are obtained by means of the complex scaling procedure which discretizes the continuum of the recoiling positronium and allows the extraction of the leptonic transition matrix element at the energies satisfying the energy conservation.

At very low energies, the rate for elastic collisions behaves as $\lambda_{el} \sim k \sim \sqrt{T}$ and the rate for inelastic collisions λ_{inel} is constant, which implies existence of a certain limiting temperature below which $\lambda_{inel} > \lambda_{el}$ and consequently the annihilation (and loss of antihydrogen) dominate the cooling process.

The size of σ_{el}, σ_{inel} and the ratio $\lambda_{inel}/\lambda_{el}$ will decide the lowest temperature attainable in collisional cooling of antihydrogen, and its density (depending on losses in annihilation occuring largely due to inelastic rearrangement collisions).

During the workshop we will present the cross sections for the rearrangement collision (eq. 1) and discuss the implications of our results on the prospects of trapping and cooling antihydrogen.

References

[1] M.H. Holzscheiter *et al.*, Nuc. Phys. B (Proc. Suppl.) **56** A, 336 (1997).

[2] M. Charlton *et al.*, Phys. Rep. **67**, 241 (1994).

[3] D.L. Morgan and V.W. Hughes, Phys. Rev. D **2**, 1389 (1970).

[4] W. Kolos, D.L. Morgan, D.M. Schrader and L. Wolniewicz, Phys. Rev. A **11**, 1792 (1975).

	Morning session(1)		Morning session(2)		Afternoon Session(1)		Afternoon Session(2)	Evening Session
18th								19:30- **Welcome drink at Shinagawa Prince Hotel**
19th	9:00-10:45 (T.Yamazaki) **K.Komaki** (30min) Antimatter Science with Slow Antiprotons **H.Knudsen**(30min) Experimental data on ionization and energy loss for antiprotons colliding with matter **P.Krstic** (30min) Ionization of ions and atoms by slow antiprotons **A.Igarashi**(15min) Ionization of atomic hydrogen with antiprotons	coffee	11:10-13:00 (H.Knudsen) **R.Hayano** (30min) Laser spectroscopy of protonium **J.S.Cohen** (30min) Isotope effects on antiproton capture **M.Fujiwara** (30min) Muon catalyzed fusion studies with a muonic hydrogen beam at TRIUMF **K.Ohtsuki** (20min) Antiprotonic lithium atom ; formation, energy levels and stability	lunch	14:20-16:00 (A.Mohri) **K.Fine** (40min) Nonneutral plasmas and antihydrogen production **T.Ichioka** (30min) Status report on the ASACUSA antiproton trapping system **H.Totsuji** (30min) Two-Component Nonequilibrium Nonneutral Plasma in Penning-Malmberg Trap	16:00- **Z a z e n k a i at Sojiji**
20th	9:00-10:50 (J.Eades) **M.Hori**(30min) High-precision, two-photon laser spectroscopy of antiprotonic helium atoms and other experiments using ultra-low density targets **Y.Kino** (30min) Non-Adiabatic High-Precision Calculation of Antiprotonic Helium Atomcule and Determination of Antiproton Mass **V. I.Korobov** (30min) Spectroscopy of the antiprotonic atomcule **T.Koike**(20min) Nuclear absorption process in antiprotonic helium atoms	coffee	11:20-12:40 (T.Watanabe) **G.Ya.Korenman** (30min) Collisions of antiprotonic atomcules with He atoms **D.Bakalov** (30min) Density shift and broadening of the transition lines in antiprotonic helium **T.Azuma** (20min) Does a solvated antiproton exist ?	lunch	14:00-15:30 (N.Toshima) **H.Schmidt-Boecking** (30min) Comparison of multi-differential ionization cross sections in fast antiproton and proton on Helium collisions — A proposal for future studies with a table sized PBAR-storage ring **C.D.Lin** (30min) Ionization of H and He atoms by antiprotons revisited **A.Kover** (30min) Post Collision Interaction at Proton, Antiproton - Atom Collisions	coffee	16:00-17:10 (M.Kamimura) **R.Schuch** (20min) An accurate measurement of the p mass using highly charged ions in a Penning trap **E.Morenzoni** (30min) A new low energetic muon beam and its applications **N.Kabachnik** (20min) Channeling of slow antiprotons	19:00- **Banquet at Shinagawa Prince Hotel**
21st	9:00-10:40 (D.Horvath) **M.Holzscheiter** (30min) Tests of CPT, Lorenz Invariance and the WEP with Antihydrogen **R.Schuch** (20min) Making Hbar by recombination in a Penning trap **S.Schippers** (30min) Recombination of H-like ions with electrons: a testing ground for the formation of anti-hydrogen? **P.Froelich** (20min) Hydrogen - Antihydrogen Collisions	coffee	11:00-12:30 (J.Eichler) **Panel Discussion** Antihydrogen Production & Spectroscopy **M.Inokuti** (20min) Concluding Remarks					

LIST OF PARTICIPANTS

Azuma Toshiyuki
University of Tsukuba
Institute of Applied Physics
Ten-nohdai 1-1-1, Tsukuba
Ibaraki, 305-8573
Japan
TEL:+81-298-53-5301
FAX:+81-298-53-5205
azuma@bk.tsukuba.ac.jp

Bakalov Dimitre D.
Bulgarian Academy of Sciences
Institute for Nuclear Research and Nuclear Energy
blvd. Tsarigradsko chaussee 72
Sofia, 1784
Bulgaria
TEL: +359-2-891605
FAX:+359-2-9753619
dbakalov@inrne.acad.bg

Cohen James S.
Los Alamos National Laboratory
Group T-4, MS B212
Los Alamos, NM 87545
USA
TEL: +1-505-667-5982
FAX:+1-505-665-6229
cohen@lanl.gov

Eades John
CERN
EP Division
1211 Geneva 23
Switzerland
TEL:+41-22-767-4273
FAX:+41-22-767-3500
John.Eades@cern.ch

Eichler Jörg
Hahn-Meitner-Institut Berlin
Glienicker Str. 100
Berlin 14109
Germany
TEL:+4930-8062-2079
FAX:+4930-8062-2098
eichler@hmi.de

Fine Kevin Sanford
CERN
Division EP
1211 Geneva 23
Switzerland
TEL:+41-79-201-4032
FAX:+41-22-767-8955
Kevin.Fine@cern.ch

Froelich Piotr
Uppsala University
Department of Quantum Chemistry

Box 518, 75120 Uppsala
Sweden
TEL:+46-18-4713262
FAX:+46-18-502402
piotr@kvac.uu.se

Fujiwara Makoto C.
University of Tokyo
Department of Physics
7-3-1 Hongo, Bunkyo-ku
Tokyo, 113-0033
Japan
TEL:+81-3-5841-4234
FAX:+81-3-5841-7642
fujiwara@nucl.phys.s.u-tokyo.ac.jp

Hayano Ryugo
University of Tokyo
Department of Physics
7-3-1 Hongo, Bunkyo-ku
Tokyo, 113-0033
Japan
TEL:+81-3-5841-4235
FAX:+81-3-5481-7462
hayano@phys.s.u-tokyo.ac.jp

Higaki Hiroyuki
University of Tokyo
Institute of Physics
3-8-1 Komaba, Meguro-ku
Tokyo, 153-8902
Japan
TEL:+81-3-5454-6988
FAX:+81-3-5454-6515
higaki@radphys4.c.u-tokyo.ac.jp

Holzscheiter Michael H.
Los Alamos National Laboratory
MS H803
Los Alamos, NM 87545
USA
TEL:+1-505-665-0491
FAX:+1-505-665-4121
mhh@lanl.gov

Hori Masaki
Univerisity of Tokyo
Department of Physics
7-3-1 Hongo, Bunkyo-ku
Tokyo, 113-0033
Japan
TEL:+81-3-5841-4236
FAX:+81-3-5841-7642
mhori@nucl.phys.s.u-tokyo.ac.jp

Horvath Dezso
Research Institute for Particle and Nuclear Physics
Konkoly-Thege 29-33
Budapest , H-1121
Hungary
TEL:+36-1-395-9220
FAX:+36-1-395-9151
horvath@rmki.kfki.hu

Ichioka Toshiyasu
Univerisity of Tokyo
Institute of Physics
3-8-1 Komaba, Meguro-ku
Tokyo, 153-8902
Japan
TEL:+81-3-5454-6515
FAX:+81-3-5454-6515
itchy@radphys4.c.u-tokyo.ac.jp

Igarashi Akinori
Miyazaki University
Faculty of Engineering
1-1 Gakuenkibanadainishi, Miyazaki-shi
Miyazaki, 889-2192
Japan
TEL:+81-985-58-7374
FAX:+81-985-58-7376
igarashi@phys.miyazaki-u.ac.jp

Inokuti Mitio
Argonne National Laboratory
9700 South Cass Ave.
Argonne 60439
USA
TEL:+1-630-252-4186
FAX:+1-630-252-3903
inokuti@anl.gov

Kabachnik Nikolay
University of Bielefeld
Faculty of Physics
Bielefeld D-33615
Germany
TEL:+49-521-106-5353
FAX:+49-521-106-6002
nkabach@physik.uni-bielefeld.de

Kambara Tadashi
RIKEN
Atomic Physics Lab.
Hirosaw a2-1, Wako-shi
Saitama, 351-0198
Japan
TEL:+81-48-467-9485
FAX:+81-48-462-4644
kambara@rikaxp.riken.go.jp

Kamimura Masayasu
Kyushu University
Department of Physics
Fukuoka 812-8581
Japan
TEL:+81-92-642-2560
FAX:+81-92-642-2560
kami2scp@mbox.nc.kyushu-u.ac.jp

Kino Yasushi
Tohoku University
Department of Chemistry
Aramaki, Aoba-ku
Sendai, 980-8578
Japan
TEL:+81-22-217-6596
FAX:+81-22-217-6597
kino@mail.cc.tohoku.ac.jp

Knudsen Helge
Aarhus University
Institute of Physics and Astronomy
Ny Munkegade
DK - 8000,Aarhus C
Denmark
TEL:+45-8942-3607
FAX:+45-8612-0740
hk@ifa.au.dk

Koike Takahisa
High Energy Accelerator Reserch Organization, KEK
Tanashi Branch, Theory Group
3-2-1 Midori-cho, Tanashi
Tokyo, 188-8501
Japan
TEL:+81-424-69-9537
FAX:+81-424-62-0763
tkoike@tanashi.kek.jp

Kojima Takao M.
RIKEN
Atomic Physics Laboratory
Hirosawa 2-1, Wako-shi
Saitama, 351-0198
Japan
TEL:+81-48-467-9486
FAX:+81-48-462-4644
kojima@rikaxp.riken.go.jp

Komaki Ken-ichiro
University of Tokyo
Institute of Physics
3-8-1 Komaba, Meguro-ku
Tokyo, 153-8902
Japan
TEL:+81-3-5454-6514
FAX:+81-3-5454-6998
komaki@phys.c.u-tokyo.ac.jp

Korenman Grigori
Moscow State University
Institute of Nuclear Physics
Moscow 119899
Russia
TEL:+7-095-9392513
FAX:+7-095-9390896
korenman@anna19.npi.msu.su

Korobov Vladimir I.
JINR
Dubna, 141980
Russia
TEL:+7-09621-63906
FAX:+7-09621-66666
korobov@nu.jinr.ru

Köver Akos
Institute of Nuclear Research of
Hung. Acad. Sci (ATOMKI)
P.O.B. 51. Debrecen. H-4001
Hungary
TEL:+36-52-417-266
FAX:+36-52-416-181
a.kover@atomki.hu

Krstic Predrag
Oak Ridge National Laboratory
Physics Division
P.O. Box 2008
Oak Ridge, 37831-6372
USA
TEL:+1-423-574-4701
FAX:+1-423-574-3745
krstic@mail.phy.ornl.gov

Kuroda Naofumi
University of Tokyo
Institute of Physics
3-8-1Komaba, Meguro-ku
Tokyo, 153-8902
Japan
TEL:+81-3-5454-6515
FAX:+81-3-5454-6515
kuroda@radphys4.c.u-tokyo.ac.jp

Lin Chii-Dong
Kansas State University
Cardwell Hall, Department of Physics
Manhattan, KS 66506
USA
TEL:+1-785 532 1617
FAX:+1-785 532 6806
cdlin@phys.ksu.edu

Machtoub Ghada Hafez
University of Electro-Communications
Chofugaoka 1-5-1, Chofu-shi
Tokyo, 182-8585
Japan
TEL:+81-424-43-5458
FAX:+81-424-43-5505
ghada@power1.pc.uec.ac.jp

Merrison Jonathan Peter
Aarhus University
Institute for Physics and Astronomy
Ny Munkegade, Aarhus 8000C
Denmark
TEL:+45-8942- 4876
merrison@dfi.aau.dk

Mohri Akihiro
RIKEN
Atomic Physics Lab.
Hirosawa2-1, Wako-shi
Saitama 351-0198
Japan
TEL:+81-48-467-9490
FAX:+81-48-462-4644
akimohri@ip.media.kyoto-u.ac.jp

Morenzoni Elvezio A.
Paul Scherrer Institute
CH-Villigen PSI
Switzerland
TEL:+41-56-310-36-70
FAX:+41-56-310-32-94
morenzoni@psicl0.psi.ch

Morishita Toru
University of Electro-Communications
Chofu-ga-oka 1-5-1, Chofu-shi
Tokyo, 182-8585
Japan
TEL:+81-424-43-5458
FAX:+81-424-43-5505
toru@pc.uec.ac.jp

Nakai Yoichi
RIKEN
Atomic Physics Lab.
Hirosawa 2-1, Wako-shi
Saitama 351-0198
Japan
TEL:+81-48-467-9487
FAX:+81-48-462-4644
nakai@rikaxp.riken.go.jp

Ohtsuki Kazumasa
University of Electro-Communications
Chofu-shi 182-8585
Japan
TEL:+81-424-43-5558
FAX:+81-424-43-5563
ohtsuki@e-one.uec.ac.jp

Oshima Nagayasu
RIKEN
Atomic Physics Lab.
Hirosawa 2-1, Wako-shi
Saitama, 351-0198
Japan
TEL:+81-48-467-9483
FAX:+81-48-462-4644
noshima@postman.riken.go.jp

Sakaguchi Jun
University of Tokyo
Department of physics
7-3-1 Hongo, Bunkyo-ku
Tokyo, 113-0033
Japan
jun@nucl.phys.s.u-tokyo.ac.jp

Schippers Stefan
Strahlenzentrum der
Justus-Liebig-Universität
Institut für Kernphysik
Leihgesterner Weg 217
Giessen 35392
Germany
TEL:+49-641-99-15203
FAX:+49-641-99-15009
Stefan.E.Schippers@strz.uni-giessen.de

Schmidt-Böcking Horst
University Frankfurt
Institut für kernphysik
August-Euler-Str.6
D-60486 Frankfurt
Germany
TEL:+49-69-798-24252
FAX:+49-69-798-24212
schmidtb@ikf.uni-frankfurt.de

Schuch Reinhold
Stockholm University
Atomic Physics
Frescativ. 24
Stockholm, S-10405
Sweden
TEL:+46-8-161046
FAX:+46-8-158674
schuch@msi.se

Takekawa Michiya
RIKEN
Atomic Physics Lab.
Hirosawa2-1, Wako-shi
Saitama, 351-0198
Japan
TEL:+81-48-467-9483
FAX:+81-48-462-4644
mtake@postman.riken.go.jp

Teranishi Yoshiaki
RIKEN Atomic Physics
Hirosawa 2-1, Wako-shi
Saitama, 351-0198
Japan
TEL:+81-48-467-9484
FAX:+81-48-462-4644
teran@postman.riken.go.jp

Torii Hiroyuki A.
University of Tokyo
Institute of Physics
3-8-1 Komaba, Meguro-ku
Tokyo, 153-8902
Japan
TEL:+81-3-5454-6545
FAX:+81-3-5454-6515
torii@radphys4.c.u-tokyo.ac.jp

Toshima Nobuyuki
University of Tsukuba
Institute of Materials Science
Tennoudai 1-1-1, Tsukuba
Ibaraki , 305-8573
Japan
TEL:+81-298-53-5317
FAX:+81-298-55-7440
toshima@bk.tsukuba.ac.jp

Totsuji Hiroo
Okayama University
Faculty of Engineering
Tsushimanaka 3-1-1
Okayama, 700-8530
Japan
TEL:+81-86-251-8141
FAX:+81-86-251-8262
totsuji@elec.okayama-u.ac.jp

Wada Michiharu
RIKEN
Atomic Physics Lab.
Hirosawa 2-1, Wako-shi
Saitama, 351-0198
Japan
TEL:+81-48-467-9487
FAX:+81-48-462-4644
mw@postman.riken.go.jp

Watanabe Tsutomu
International Christian University
Ohsawa 2-10-3 Mitaka-shi
Tokyo 181-8585
Japan
TEL:+81-422-33-3249
FAX:+81-422-33-1449
tsutomu@icu.ac.jp

Yamaguchi Hidetoshi
University of Tokyo
Department of Physics
7-3-1 Hongo,Bunkyo-ku
Tokyo, 113-0033
Japan
TEL:+81-3-5841-4236
FAX:+81-3-5841-7642
yamaguti@nucl.phys.s.u-tokyo.ac.jp

Yamazaki Toshimitsu
JSPS
5-3-1 koji-machi, Chiyoda-ku
Tokyo, 102-0083
Japan
TEL:+81-3-3263-1721
FAX:+81-3-3237-8238
yamazaki@tkynx0.phys.s.u-tokyo.ac.jp

Yamazaki Yasunori
University of Tokyo
Institute of Physics
3-8-1Komaba, Meguro-ku
Tokyo, 153-8902
Japan
TEL:+81-3-5454-6521
FAX:+81-3-5454-6433
yasunori@phys.c.u-tokyo.ac.jp

Yoshiki Franzen Ken
University of Tokyo
Institute of Physics
3-8-1 Komaba, Meguro-ku
Tokyo, 153-8902
Japan
ken@atom.kth.se